

AN ABSTRACT OF THE THESIS OF

William C. Faye for the degree of Master of Science  
in Department of Mechanical Engineering presented on February 22,  
1982.

Title: NO<sub>x</sub> Emissions From a Gas Turbine as a Function of Fuel Bound  
Nitrogen and Other Variables

Abstract approved: Redacted for Privacy  
Richard Boubel

Emissions of oxides of nitrogen from a small (15 kW) turbine generator burning high fuel bound nitrogen fuels were measured by a chemiluminescence method. Kerosene was used as the base fuel and pyridine was added to achieve different fuel bound nitrogen levels. Mixtures of 0.0%, 0.5%, and 1.0% (by weight) of nitrogen were tested.

Combustion chamber temperatures were measured with a shielded type K thermocouple inserted through the combustor can.

The NO<sub>x</sub> values found were slightly lower than other studies using similar combustors. However, this can be attributed to lower combustion temperatures and to differences in fuels and combustor inlet conditions. When the NO<sub>x</sub> values were plotted against temperature they were found to fit a straight line plot quite well. This is in agreement with other subscale combustor test results.

The production rate of  $\text{NO}_x$  versus fuel bound nitrogen content was found to be less dependent on nitrogen content at higher temperatures than at lower values. The overall rate of production of  $\text{NO}_x$  was still higher at the higher temperatures.

NO<sub>x</sub> Emissions from a Gas Turbine as a Function of  
Fuel-Bound Nitrogen and Other Variables

by

William Faye

A THESIS

submitted to

Oregon State University

February 22, 1982

in partial fulfillment of  
the requirements for the  
degree of  
Master of Science  
June 1982

APPROVED:

Redacted for Privacy

\_\_\_\_\_  
Professor of Mechanical Engineering in charge of major

Redacted for Privacy

\_\_\_\_\_  
Head of Department of Mechanical Engineering

Redacted for Privacy

\_\_\_\_\_  
Dean of Graduate School

Date thesis is presented

FEB. 22, 1982

Typed by Mary Ann Airth for

William Faye

## ACKNOWLEDGEMENTS

I would like to thank all those who have helped make this work possible. Lack of space, however, limits me to just a few. Dr. Boubel deserves thanks for his advice and assistance throughout the experimentation and writing of this report. Thanks go to Dr. Mingle for his help in setting up the equipment and his help in understanding its workings and difficulties. The U.S. Air Force also receives my thanks for supplying the financial and material backing for this research. I would also like to thank my typist, Sadie Airth, for her patience and skill in the preparation of this paper. A special thanks go to my fiancée, Kathy, for without the incentive she has given me I might never have finished. Finally, I would like to thank God, without the tools and guidance He has given me I would never had made it here.

## TABLE OF CONTENTS

INTRODUCTION	1
PURPOSE	4
THEORY	5
Thermal NO	5
Prompt NO	6
Fuel Bound Nitrogen	7
NO <sub>2</sub> Formation	8
APPARATUS	10
PROCEDURES	23
RESULTS	25
CONCLUSIONS	44
REFERENCES	45
BIBLIOGRAPHY	48
APPENDICES	51
1) Test of Scott NO <sub>x</sub> Analyzer Accuracy	52
2) Beckman CO <sub>2</sub> Analyzer Calibration Curve	52
3) Calculation of Required Additive Volume for a Given Weight Percent of Mixed Fuel	54
4) Gas Turbine Data Sheet	58
5) Test Operating Procedure	59
6) NO <sub>x</sub> Values from Data Sheets	61
7) Determination of Combustor Inlet Temperature	64
8) Weight Percent of an Element in a Fuel Mixture	66
9) Fuel Density Calculations	70
10a) Calculation of A/F Ratios by Direct Measurement	74
10b) Calculation of the Percent Theoretical Air in Combustion from Combustion Stoichiometry	77
11) Calculation of Heat of Formation of Kerosene	80
12) Estimate of the Adiabatic Flame Temperature	82

## LIST OF FIGURES

<u>Figure</u>	<u>Page</u>
1. Gas turbine generator	11
2. Combustor can assembly	11
3. Fuel control panel	12
4. Sample conditioning system	14
5. Scott NO <sub>x</sub> Analyzer	14
6. Schematic Scott NO <sub>x</sub> Analyzer	15
7. CO <sub>2</sub> analyzer, chart recorder and electrical loading device	17
8. Digital temperature indicator	18
9. Combustor flame temperature thermocouple	20
10. Rear view of turbine-compressor	20
11. Wet and dry bulb measurement	21
12. Room set up	21
13. North Star Horizon computer	22
14. Adjusted NO <sub>x</sub> vs. measured flame temperature	32
15. NO <sub>x</sub> emissions for SRC recycle solvent and its surrogate	33
16. NO <sub>x</sub> emissions for H-coal (ATM-OVHD) 366-533K and its surrogate	33
17. NO <sub>x</sub> emissions for SRC light organic, and its surrogate	33
18. NO <sub>x</sub> emissions for SRC wash solvent and its surrogate	33

19. Adjusted $\text{NO}_x$ vs. Adiabatic flame temperature	36
20. Adjusted $\text{NO}_x$ vs. Air/fuel ratio	38
21. $\text{NO}_x$ vs. fuel bound nitrogen	40

## LIST OF TABLES

<u>Table</u>	<u>Page</u>
I. $\text{NO}_x$ Information - Measured and Derived	26
II. Adjusted $\text{NO}_x$ vs. Measured Flame Temperature	31
III. Adjusted $\text{NO}_x$ vs. Adiabatic Flame Temperature	37
IV. Adjusted $\text{NO}_x$ vs. Air/Fuel Ratio and Theoretical Air	37
V. $\text{NO}_x$ vs. Fuel Bound Nitrogen	41
VI. $\text{NO}_x$ vs. Fuel Bound Nitrogen Least Squares Curve Fits	41

# $\text{NO}_x$ Emissions from a Gas Turbine as a Function Fuel-Bound Nitrogen and Other Variables

## INTRODUCTION

The study and control of oxides of nitrogen ( $\text{NO}_x$ ) formed during combustion processes, has gained new emphasis in the past few years as their effect on the environment becomes more well known. These effects are concentrated into two main areas, the formation of photochemical oxidants which are a cause of smog, and their combination with water to form dilute nitric acid, which precipitates out as acid rain.

The contribution of  $\text{NO}_x$  to smog is primarily that of a producer of free radicals which combine with oxygen and hydrocarbons to form Ozone and complex hydrocarbon chains.

The  $\text{NO}$  combines with oxygen in the atmosphere to produce  $\text{NO}_2$ . This  $\text{NO}_2$ , along with  $\text{NO}_2$  emitted in the initial combustion reaction, is acted upon by ultraviolet light and breaks down into  $\text{NO}$  and an oxygen radical. This oxygen radical then can combine with diatomic oxygen to form ozone, which is a strong oxidizer. The ozone reacts with hydrocarbons in the atmosphere, forming many of the irritants which cause irritation of the eyes, nose and throat, and headaches.<sup>1</sup> The ozone also reacts strongly with many substances causing rapid degradation of rubber, nylon, and other fabrics and synthetics.



Acid rain also affects buildings, structures and statues by reacting with the stone and construction materials to etch or weaken them. Other effects of acid rain include rapid corrosion of paints and finishes on houses and automobiles, the dissolving of lead solder on piping (and its introduction into drinking water), and the dissolving and introduction of mercury into lakes and streams, and thence into the food chain.

It is mainly for these reasons, their contribution to smog and to acid rain, that  $\text{NO}_x$  emissions have come under closer study and tighter control by the Environmental Protection Agency.

## PURPOSE

Studies by the Air Force in the late 1970's indicated that it would be desirable for the United States to develop its shale oil reserves as a source of military jet fuel.<sup>6</sup> This fuel would be readily accessible and is considered sufficient to supply our needs in the event of national emergency.

Shale oil and synthetic fuels from coal have a higher nitrogen content, in the form of ammonia and pyridine compounds, than do most petroleum derived fuels. For this reason, it was of interest to the Air Force to see what effect this high nitrogen content would have on NO<sub>x</sub> emissions.

## THEORY

This section gives a brief overview of the theories and mechanisms which have been proposed as the major pathways of  $\text{NO}_x$  production in combustion systems. For a more complete background in this area, the reader is referred to the book, Combustion, by Irvin Glassman<sup>7</sup>, from which most of this section was taken.

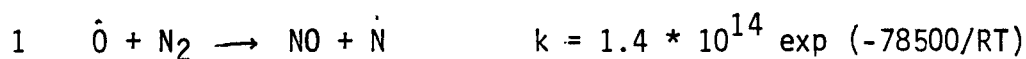
In fuel injection systems such as a gas turbine, the fuel droplets burn as diffusion flames near the stoichiometric air fuel ratio. It is only after these fuels are completely vaporized and mixed that they reach the final air fuel ratios indicated by calculations. As a result, the reactions take place at a higher temperature than would be anticipated and the resulting concentrations of  $\text{NO}_x$  are higher than would be expected from overall mixture ratios.

Much of the  $\text{NO}_x$  formed is in the form of nitrous oxide  $[\text{NO}]$  with significantly smaller concentrations of  $\text{NO}_2$  and minor amounts of  $\text{N}_2\text{O}_4$ . For the moment we shall concentrate on production of  $\text{NO}$  in nitrogen free fuels. We will then address fuel bound nitrogen kinetics and the generation of  $\text{NO}_2$ .

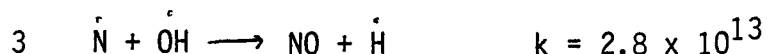
### Thermal NO

$\text{NO}$  from the combustion of nitrogen free fuels is highly temperature dependent and formed primarily by what is called the Zeldovich Mechanism.

First proposed by the Russian scientist Ya. B. Zeldovich in 1946, this model postulates that oxygen atoms are first formed from the thermal dissociation of  $O_2$  or by hydrogen attack on atmospheric oxygen. This free oxygen atom then combines with atmospheric nitrogen as shown below.



Some later researchers have included the reaction

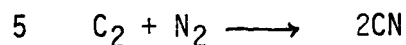
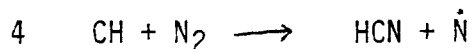


although this is felt to contribute to a much lesser extent.

Because of its high activation energy equation 1 is slow and acts as the control on the reaction. Because of the slowness of the reaction it was thought that all of the NO was formed in the post combustion zone. However, experiments made to confirm this showed that NO concentration profiles extrapolated to the flame front did not go to zero. This lent credence to arguments that reactions other than the Zeldovich mechanism also contributed to NO production.

### Prompt NO

The NO formed in the combustion zone has been called Prompt NO. C.P. Fenimore discovered that Prompt NO is only found in the flames of hydrocarbons. This observation led to the following reaction scheme involving a hydrocarbon species and atmospheric nitrogen.



The N atoms could then form NO partially by the Zeldovich mechanism (equations 1 and 2) and the 2CN could form NO by reaction with diatomic oxygen or by attacking an oxygen atom.

It has also been theorized that if the O atom concentration in the reaction zone were much greater than the equilibrium levels, then the Zeldovich mechanism could also account for the prompt NO.

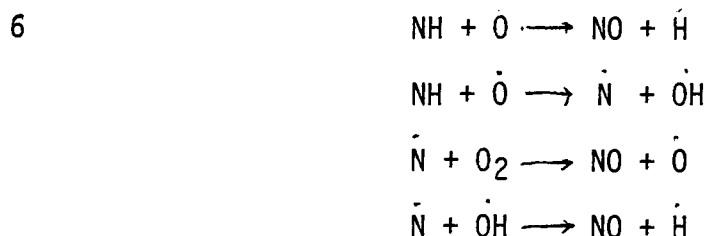
The current feeling is that both these mechanisms hold true and that which predominates depends on the flame temperatures and on the stoichiometry. In the low temperature regions the Fenimore mechanism is felt to control the production while in the high temperature areas the Zeldovich mechanism predominates due to high oxygen atom production.

### Fuel Bound Nitrogen

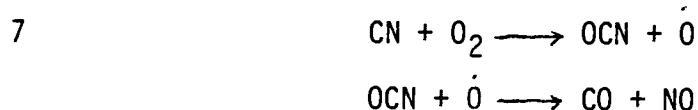
When nitrogen is present in the fuel, the NO emissions increase dramatically. The chemical mechanisms for this conversion are not completely determined as yet, however a number of possible mechanisms have been suggested.

The fuel nitrogen compounds probably undergo thermal decomposition to low molecular weight nitrogen compounds or radicals prior to combustion. These might include  $\text{NH}_2$ , HCN, CN,  $\text{NH}_3$ , NH, etc.

Some suggested qualitative conversion routes for NH would be:



A conversion route which has been suggested for CN is:



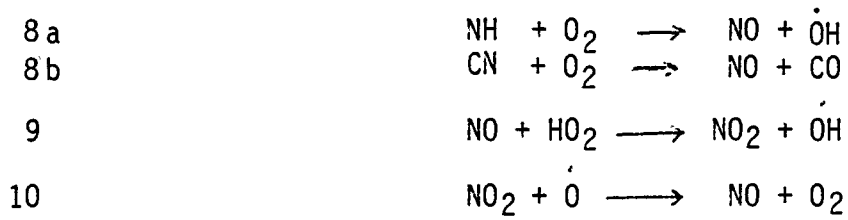
These reactions are quite fast and occur at approximately the same rate as the energy release during combustion.

### NO<sub>2</sub> Formation

NO<sub>2</sub> is found in significant concentrations in the exhaust gases of some combustion systems, including gas turbines. This is surprising as chemical equilibrium calculations and kinetic models would indicate that it would not be found in appreciable quantities.

Because of this discrepancy, researchers have looked into NO<sub>2</sub> production and found that it is formed in the visible regime of all air flames. In most cases however, it is rapidly converted to NO in the post flame zone.

The following scheme has been suggested for the production and consumption of NO<sub>2</sub> in fuels containing nitrogen.



Reaction 9 is important as there can be significant amounts of  $\text{HO}_2$  in the early parts of the flame.

It is also important to note that the reaction rate of equation 10 is two orders of magnitude slower than that of equation 9. Because of this, it is quite possible that reaction 10 is quenched before completion in some systems, such as gas turbines. This would account for the higher levels of  $\text{NO}_2$  encountered in such systems.

## APPARATUS

The main power plant for this project was an Airesearch Manufacturing Company Gas Turbine Generator, Model No. GTGE30-23 with a turbine engine, model No. GTP30-40. It was a self contained unit capable of generating up to 15 kw of electricity of AC or DC current. The package was fully instrumented to show output voltage, frequency, current and power, DC generator voltage, and percentage of engine rpm. Additional instrumentation had been added to show fuel pressure, compressor air pressure, combustion chamber temperature and exhaust temperature. See Figure 1.

The gas turbine system was a simple open cycle coupled turbine type, consisting of a centrifugal compressor and turbine wheel mounted on a common shaft and a combustor which exhausted into the turbine. The combustor was a single can type, as shown in Figure 2.

The turbine was speed governed by the proper metering of fuel. The fuel flow was adjusted to maintain a constant speed of 48,000 rpm under varying electrical loads.

The generator was connected to a series of resistors shown in the back corner of Figure 1. The switching box was able to give one half and full load to the generator, 6.25 kW and 15 kW, respectively. Zero load was achieved by opening the AC circuit breaker on the front panel of the turbine generator.

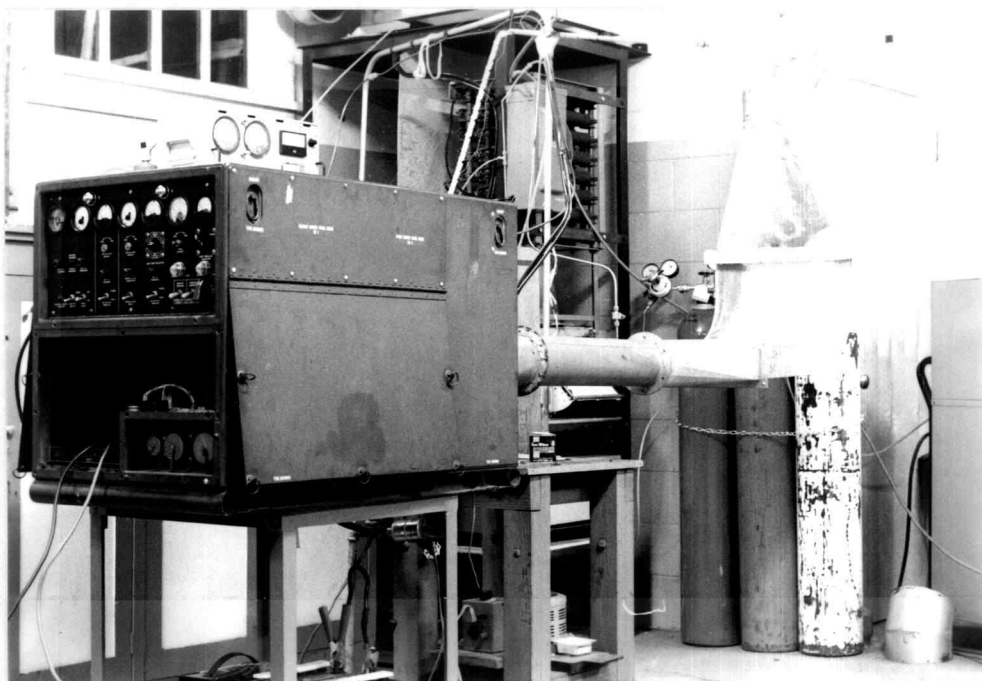


Figure 1. Gas turbine generator

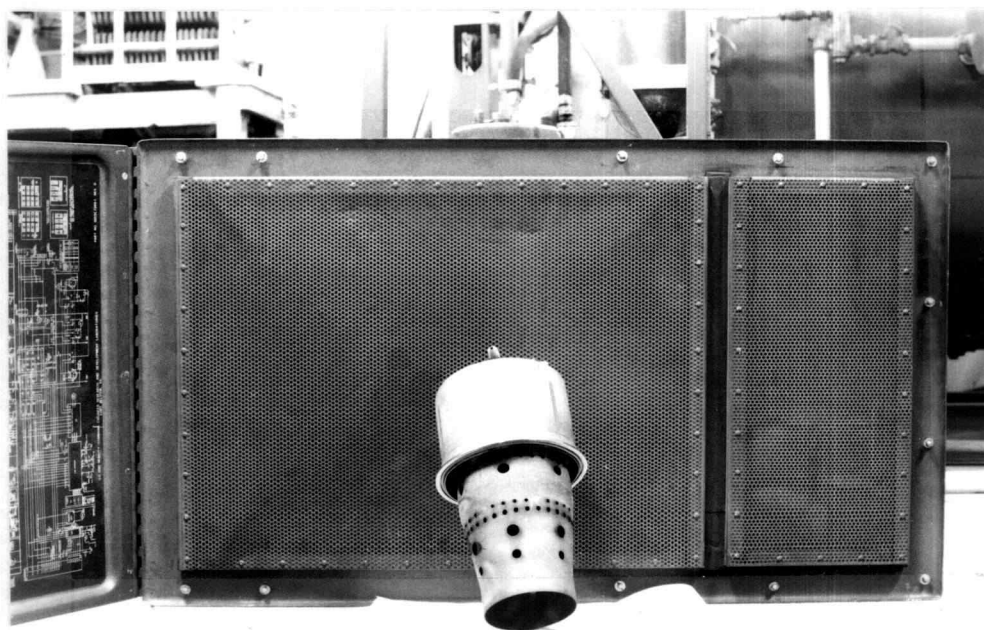


Figure 2. Combustor can assembly

The turbine was supplied with fuel stored and metered in the fuel control panel, as shown in Figure 3.

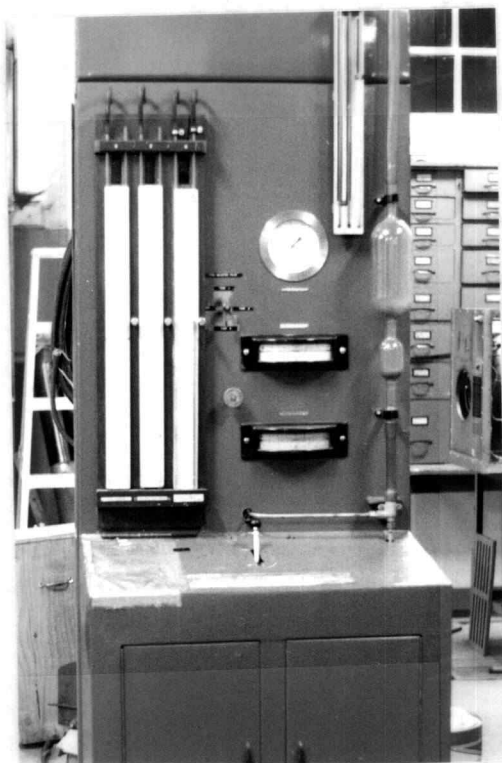


Figure 3. Fuel control panel

The control panel had three fuel tanks connected to the fuel line through a three-way valve, shown in the center. Measures of fuel flow rate were made by timing the flow of fuel through the 2000 cc burette on the right hand side of the panel.

Assuming that the 2000 cc burette volume was correct, we would estimate an accuracy to within 0.5% of our average volume flow rates. (flow at full load was 285 sec).

The flow rates of the exhaust gases were also measured, using a Dwyer Pitot Tube and manometer . These values were read as velocity pressure in inches of water. These values were then converted to the proper velocity and mass flow rates.

Due to the extreme turbulence in the exhaust duct it was difficult to estimate the accuracy of these measurements. From the results of the calculation of air fuel ratio information, and comparison with air fuel ratios derived from CO<sub>2</sub> data, the accuracy would appear to be fairly reasonable in some cases. However, overall accuracy of better than 10% of measured values cannot be assumed.

The exhaust sample was run through an AESI model SCM 7900 sample conditioning system (see Figure 4). The sample was cooled to near ambient temperatures and the particulate matter and moisture removed. The sample was then pumped at 12 psi to the analyzers.

The sample was passed to a Scott Model 325 Chemiluminescence NO/NO<sub>x</sub> analyzer which, for our study, was used entirely in the NO<sub>x</sub> mode.

This analyzer uses the light emissions produced by the reaction of NO and ozone to measure the concentration of NO in the sample gas. The intensity of the light is proportional to the flow of NO into the chamber.

In order to measure NO<sub>x</sub> (NO and NO<sub>2</sub> combined), the sample was first passed through a thermal converter kept at 500° C. This dissociated the NO<sub>2</sub> into NO and the total concentration was then read as NO. A photograph of the instrument is shown in Figure 5,

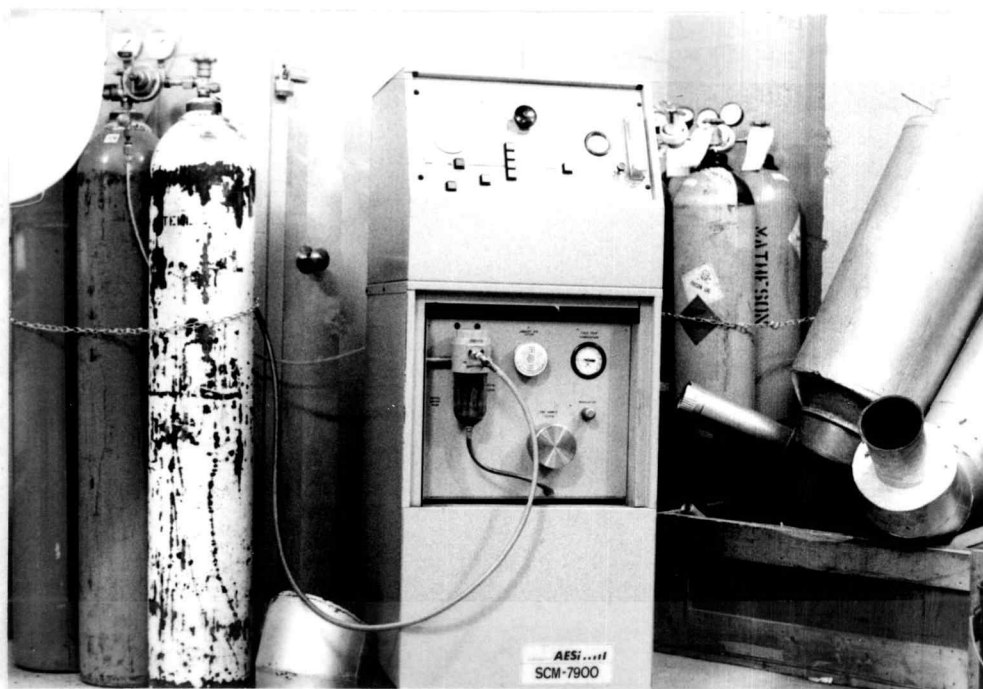


Figure 4. Sample conditioning system



Figure 5. Scott NO<sub>x</sub> analyzer

while a schematic of its major components is shown in Figure 6.

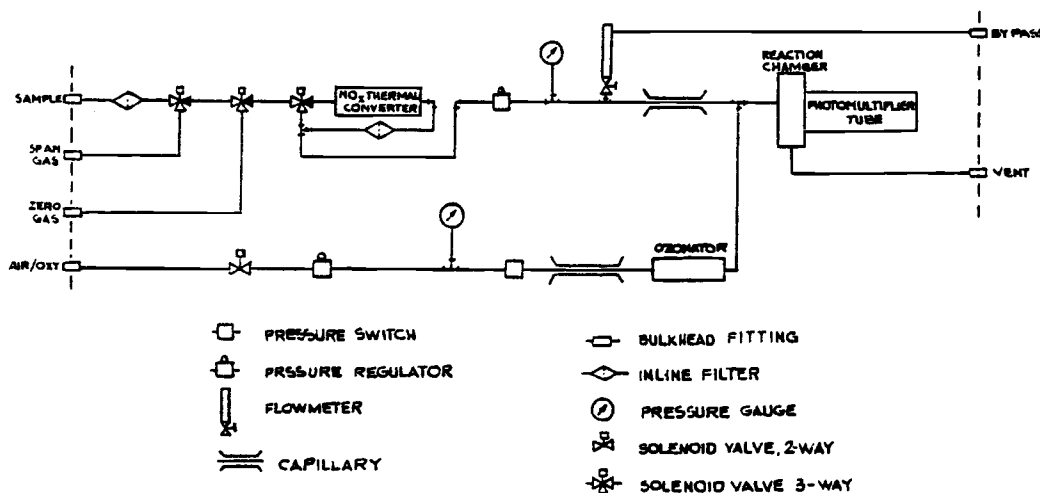


Figure 6. Schematic Scott NO<sub>x</sub> analyzer

The analyzer was capable of analyzing and measuring NO concentrations over full scale ranges of 10, 25, 100, 250, 1k, 2.5k and 10k ppm.

The stated accuracy of the instrument was within 1% of full scale for the ranges of interest.<sup>9</sup> A test of accuracy conducted on January 2, 1982, using various span gases gave values that at most are off by 5% at the outer edges of the range (see Appendix 1). This test was conducted under stable ambient conditions.

Under test conditions, changes in ambient temperature caused substantial drift in zero readings. After many extensive and unsuccessful attempts were made to try to eliminate this drift, it was decided to make measurements against frequently measured zero values. It was found that by using this method consistent results could be obtained, usually within 2 ppmv.

In some of the later runs it was noted that the relative distance between the zero and span gases was shrinking, indicating a relative change in scale. To adjust for this, span gas readings were taken periodically and measured values adjusted accordingly. An example of this procedure is given below (taken from the 0 load run 1/8/82):

Sample reading 27.5 ppmv, zero reading 3.5 ppmv

Span gas (45 ppmv) reading - 44 ppmv

Zero with span gas reading = 4.5 ppmv.

Adjustment for zero drift -  $27.5 \text{ ppmv} - 3.5 \text{ ppmv} = 24.0 \text{ ppmv}$

Span drift -  $45 \text{ ppmv actual} - (44 \text{ ppmv measured} - 4.5) = 5.5 \text{ ppmv}$

Final Adjusted Value =  $24.0 \text{ ppmv} + 5.5 \text{ ppmv} = 29.5 \text{ ppmv}$ .

Other sources of error as cited by Campbell et al.<sup>10</sup> include interference by water vapor and carbon dioxide. The error caused by these two factors was considered minimal in these tests. In the case of water vapor, our sample conditioner removed much of the moisture. The error caused by the CO<sub>2</sub> is at most 0.5 ppm and was therefore neglected.

In light of the above discussion, it was felt that the measured values can accurately approximate the true values within an error of less than 5 ppmv.

The sample gas stream was also routed to a Beckman Model 215A Infrared Analyzer to determine CO<sub>2</sub> levels. The analyzer was calibrated to read CO<sub>2</sub> concentrations of up to 5% (by volume). The calibration curve for the analyzer is given in Appendix 2.

The instruction manual<sup>11</sup> gives the accuracy of this instrument as within 1% of scale. In our case, this would translate to  $\pm 0.05\%$  CO<sub>2</sub>. Considering accuracy of the calibration curve and the curve reading techniques, an accuracy of  $\pm 0.1\%$  CO<sub>2</sub> was assumed reasonable.

Figure 7 shows a section of our instrumentation with the CO<sub>2</sub> analyzer on the bottom, the chart recorder in the center and the turbine electrical loading resistors at the top.



Figure 7. CO<sub>2</sub> analyzer, chart recorder and electrical loading device

Both the Scott 325 NO<sub>x</sub> analyzer and the Beckman 215A CO<sub>2</sub> analyzer were connected to an Esterline Angus Strip Chart recorder. The recorder had two channels.

The accuracy of the recorder was given as  $\pm 0.35\%$  of scale<sup>12</sup> which translates into  $\pm 0.35$  ppm for the  $\text{NO}_x$  values and  $\pm 0.0175\%$   $\text{CO}_2$  for the  $\text{CO}_2$  analyzer.

Additional instrumentation on our system included a series of Type K (Chromel-Alumel) thermocouples, which measured seven temperatures. Two of these, combustion flame temperature and exhaust temperature, were used in this study. The thermocouples were connected to an Omega Model 199 ten channel digital temperature indicator, as shown in Figure 8.



Figure 8. Digital temperature indicator

The accuracy of the exhaust gas measurements was conservatively estimated at  $\pm 10^\circ\text{F}$ , taking both indicator and thermocouple error

into account. The combustor flame temperature was measured with a specially modified Type K thermocouple, shown close up in Figure 9. This was designed to fit through the compressor housing and enter the final row of holes in the combustor can. These holes can be seen on the can shown in Figure 2.

The cowl protecting the thermocouple was designed to minimize the interference of radiational effects on the thermocouple and to allow free flow of exhaust gas through it. The radiational effect of having the extremely hot combustion zone just upstream, and of having the relatively cold surfaces downstream and around it, can often cause interference with true gas temperature readings.

A photograph of the back of the turbine in Figure 10 shows the combustor thermocouple entering the housing on the middle right-hand side of the casing. The exhaust temperature thermocouple can be seen in the middle foreground just beyond the flange in the exhaust duct.

The wet and dry bulb temperatures were also measured using the blower and thermometer combination shown in Figure 11.

The overall configuration of the machinery is pictured in Figure 12. The analyzers and loading system are in the back corners, the fuel measuring system in the foreground and the sample conditioning system is partially visible behind it.

Most of the calculations for this project were done with a North Star Horizon Micro-computer, using the BASIC computer language. This was a small 64 k memory computer with a CRT and hardcopy attachment. Copies of the programs used are given in the Appendices.

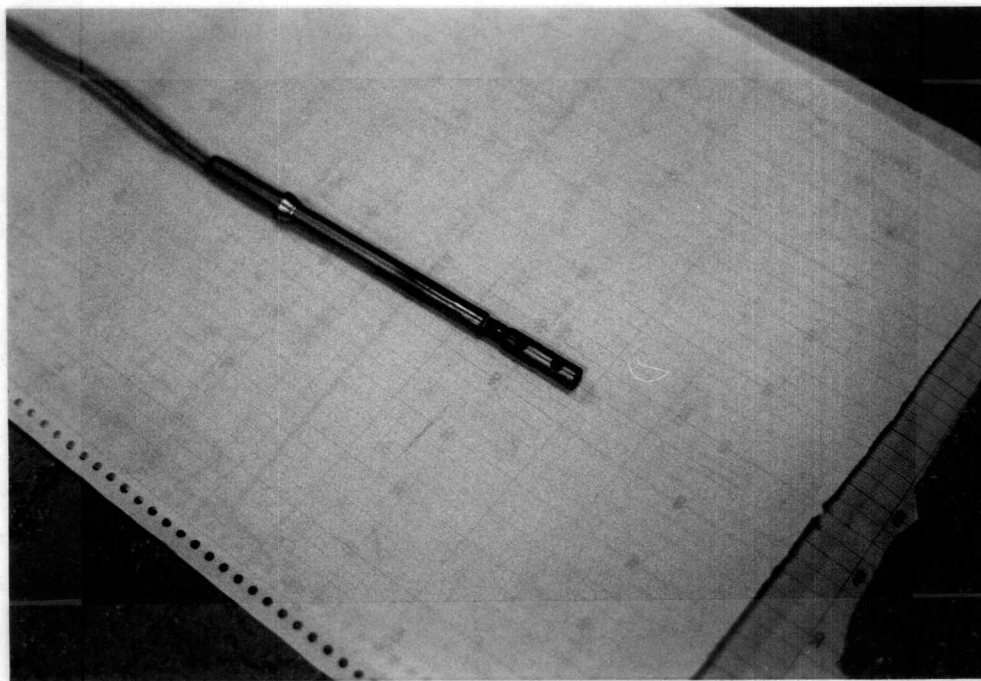


Figure 9. Combustor flame temperature thermocouple

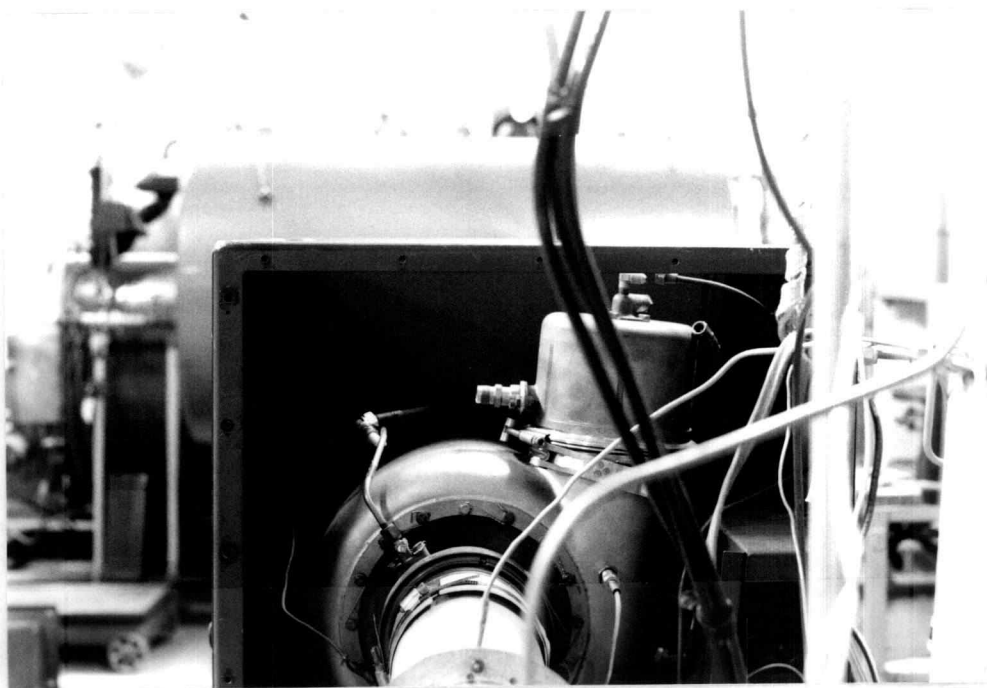


Figure 10. Rear view of turbine-compressor

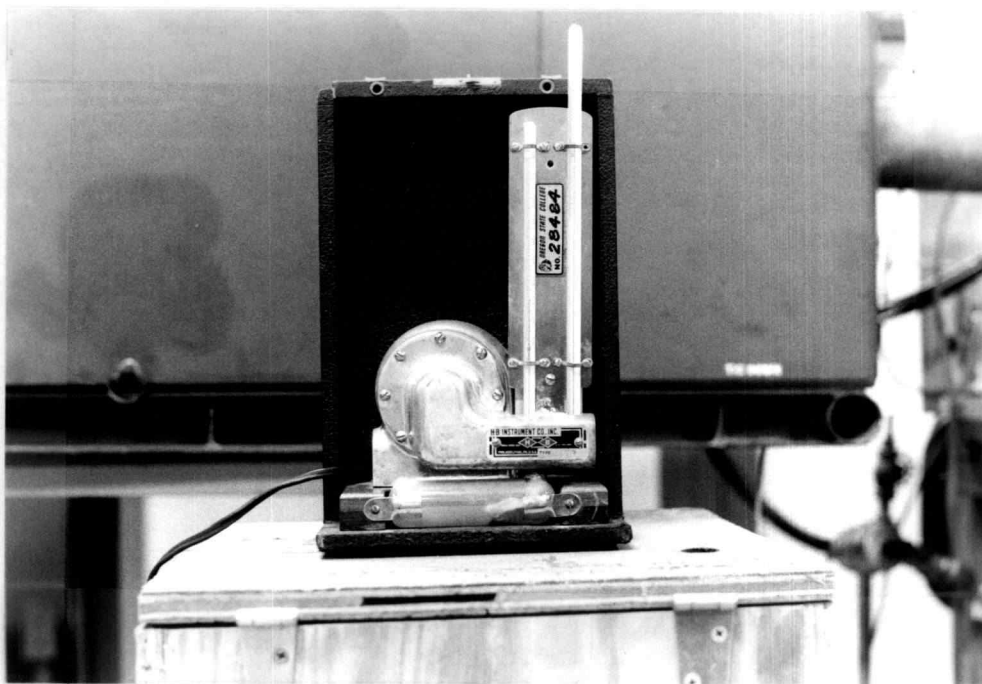


Figure 11. Wet and dry bulb measurement

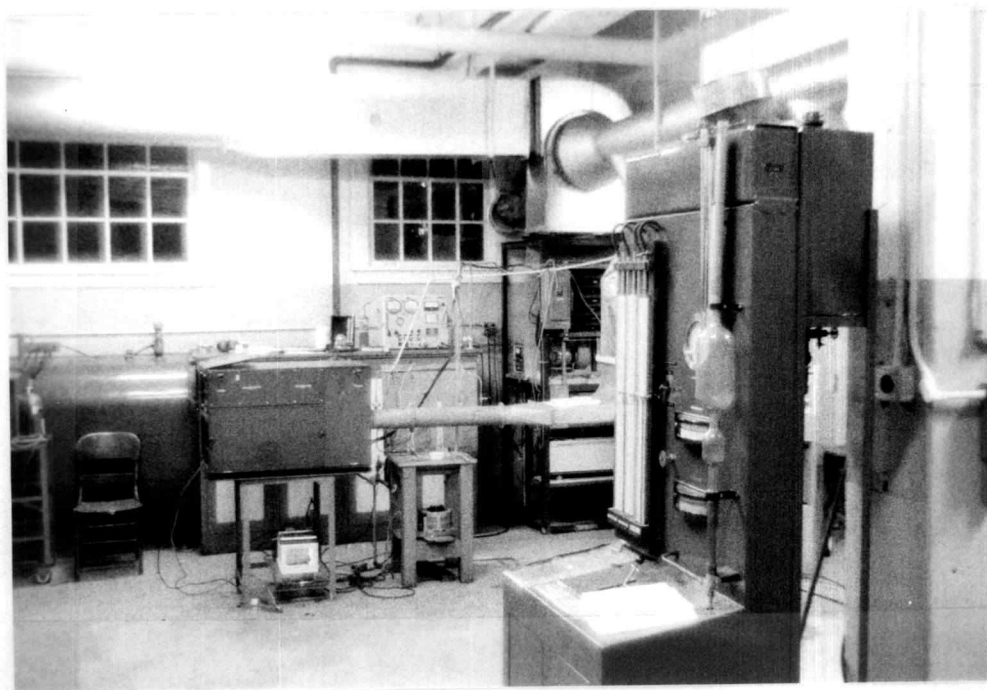


Figure 12. Room set up



Figure 13. North Star Horizon computer

## PROCEDURES

The fuels were mixed by hand in five gallon quantities and transported to the test site. Various mixtures of kerosene and pyridine were used to achieve final fuel mixtures that were of the desired weight percent nitrogen, 0.5% and 1% nitrogen by weight. (See Appendix 3 for the calculations)

The constituent fuels underwent elemental analysis conducted by R. Wielesic of the University of Oregon Chemistry Department. The samples were tested on a Perkin Elmer Model 240 carbon hydrogen nitrogen analyzer. The results obtained were: for kerosene 90.38% C and 9.09% H (weight percent), and for pyridine 17.90% N, 75.63% C and 6.68% H. The precision for this test was 0.1% for standards and 0.3 to 0.4% for pure chemicals.<sup>13</sup>

It was noted that because of this, the weight percents did not total 100%, being 99.47% for kerosene and 100.21% for pyridine. It was decided to adjust the weight percents by taking the difference between the total and 100% and adding or subtracting an equal amount from each element to achieve a total of 100%. The adjusted values used in calculations were therefore, for kerosene 90.645% C and 9.355% H, and for pyridine 17.83% N, 75.56% C, and 6.61% H.

The test procedure began by letting the analyzers warm up for one to two hours with a flow of zero gas (nitrogen) through them at the same rate as the sample and zero gas flows during the run. Both units were then calibrated using nitrogen gas as the common zero gas and

using a standard gas containing 45 ppmv of NO for the NO<sub>x</sub> analyzer and 5% CO<sub>2</sub> for the CO<sub>2</sub> analyzer. Calibration was done by adjusting the zero and gain (span) potentiometers on the instruments until the readings matched the known standards. Several alternate readings of the zero and span gases were made and the potentiometers adjusted until consistent results were obtained. Note was next made of the various ambient conditions, including barometric pressure, dry bulb temperature and wet bulb temperature.

The specific fuel to be tested was then chosen, and the turbine generator started at zero load. Experimental values were taken when a steady CO<sub>2</sub> reading was obtained, indicating steady state conditions.

At that time, note was made of the CO<sub>2</sub> concentration, fuel pressure, compressor outlet pressure, turbine exhaust and combustion chamber temperatures, and a timing was made of the flow rate of 2000 cc of fuel. The NO<sub>x</sub> concentration was also determined by alternately checking the sample and zero readings. After a number of repetitions of the sampling and zero levels, a check was also made of the span gas reading. These values were used to determine actual NO<sub>x</sub> values as indicated in the Apparatus section on the NO<sub>x</sub> analyzer.

When all the data had been gathered, the ambient temperatures were again checked and noted. The load was then changed, and the process repeated for half (6.25 kW) and full (15 kW) loads.

The Appendices contain copies of the data sheet used (Appendix 4) and the complete checklist for a run (Appendix 5).

## RESULTS

Table I contains the measured and derived variables used in the analysis of this experiment. What follows is a brief description of each of those variables.

Oxides of nitrogen were measured by the Scott Model 325 NO<sub>x</sub> analyzer, as described in the Procedural section. Relatively consistent results were obtained during each run with the largest standard deviation during a measurement series being 1.4 ppmv. The values given in the table are the mean values for each measurement series. The standard deviation around that mean is shown in parenthesis. The actual measured values for each table point are given in Appendix 6.

The mean NO<sub>x</sub> values were adjusted to combustor inlet conditions of 212°F (100°C), 2 atm, and zero absolute humidity in the exhaust gas, by the following equation.

$$11 \quad \text{NO}_{x\text{corr}} = (\text{NO}_x)_{\text{meas}}^x \left[ \exp \left[ \frac{373.15 - \left( \frac{T_{\text{in}}^{\circ\text{R}}}{1.8} \right)}{248} \right] \right] \times \left[ \frac{2 \text{ atm}}{P_{\text{in}}} \right]^{\frac{1}{2}} \times \exp(19H)$$

where  $T_{\text{in}}$  is the combustor inlet temperature in degrees Rankine,  $P_{\text{in}}$  is the combustor inlet pressure in atmospheres, and  $H$  is the absolute humidity, mass H<sub>2</sub>O/mass air, of the inlet air. An equation of this form was proposed by Lewis<sup>14</sup> to predict NO<sub>x</sub> emissions and is used by the Environmental Protection Agency to adjust its NO<sub>x</sub> standards to fit different pressure ratio engines.<sup>15</sup>

TABLE I

NO<sub>x</sub> Information - Measured and Derived

Date	Fuel (% N)	Load (Kw)	NO <sub>x</sub> (ppmv)		CO <sub>2</sub> (V%)	CO (ppmv)	T <sub>comb</sub> (°F)		T <sub>comb</sub> (°F)		T <sub>wb</sub> (°F)		H <sub>2</sub> Rel. Humidity		% P <sub>comp</sub> (atm)	T <sub>comp</sub> exit(°F)	NO <sub>x</sub> (ppmv)	A/F ratio from CO <sub>2</sub>	A/F Ratio Direct Meas.			
			σ n-1				measured	Texh Cal.	avg 1	avg 2	avg 1	avg 2	% Specific	% Abso- lute								
12/28/81	0.0	0.0	2.5 (NA)	1.35		640 <sup>+</sup>	860±10	735	471	47	48	49	50	57	53.5	68	.0058	2.222	218.75	2.61	145.35	131.00
12/28/81	0.0	9.0	8.0 (NA)	2.15	NA		1290±10	959	666	50.5	53	60	62	61	53	.0061	2.222	228.64	8.21	100.62 <sup>†</sup>	102.60	
12/30/81	0.0	9.5	9.0 (.71)	2.175	NA		1275±10	970	671	47	51	55	54	69	61.5	48	.0056	2.187	233.90	9.11	99.69 <sup>†</sup>	93.1
1/5/82	0.0	0.0	3.3 (.55)	1.40	640		860±10	748	468	50	50	51	60	55	5.55	68	.0064	2.157	214.04	3.57	140.350	143.525
1/5/82	0.0	6.25	8.3 (.29) 3 of 4 values	1.85	400		1145±10	907	611	50	55	60	70	65	43	.0056	2.157	226.45	8.61	108.503	109.786	
1/5/82	0.0	14.3	13.8 (.29)	2.60	260		1565±10	1170	817	55	56	57	70	75	72.5	34	.0058	2.225	243.55	13.61	77.817	77.539
1/6/82	0.5	0.0	9.8 (.27)	1.35	640 <sup>+</sup>		840±10	735	451	37	39	41	44	50	47	.0032	2.239	208.05	9.93	145.348	143.230	
1/6/82	0.5	6.25	24.3 (.45)	1.80	400 <sup>+</sup>		1125±15	879	583	41	43	45	50	55	52.5	44	.0037	2.239	215.29	24.46	111.478	118.203
1/6/82	0.5	15.0	41.75(.71)	2.475	260 <sup>+</sup>		1550±10	1112	764	45	45.75	46.5	55	58	56.5	43	.0041	2.274	224.09	41.20	81.756	86.968
1/7/82	1.0	0.0	30.2*(.45)	1.375	640 <sup>+</sup>		835±10	740	465	43	45.25	47.5	52	59	55.5	44	.0041	2.208	215.54	30.83	142.805	134.458
1/7/82	1.0	6.25	51.9*(.86)	1.825	400 <sup>+</sup>		1130±10	899	608	47.5	49	50.5	59	65	62	37	.0044	2.242	227.60	51.46	109.971	104.846
1/7/82	1.0	15.0	81.8**(5)	2.60	260 <sup>+</sup>		1550±10	1165	785	50.5	52.75	55	65	74	69.5	30.5	.0047	2.242	237.47	79.79	77.817	80.757
1/8/72	1.0	0.0	30.25*(.67)	1.375	640 <sup>+</sup>		860±10	726	470	47	47	47	57	58	57.5	44	.0044	2.207	218.16	30.88	142.805	138.103
1/8/82	1.0	6.25	48.2 *(1.4)	1.85	400 <sup>+</sup>		1140±10	904	603	47	48	49	58	60	59	43	.0046	2.241	223.59	48.42	108.503	106.020
1/8/82	1.0	15.5	78.4* (1.2)	2.575	260 <sup>+</sup>		1565±15	1148	788	49	50	?	61	?	62	42	.0049	2.241	227.56	78.51	78.575	81.989

\* Values adjusted to account for drift.  
 \*\* Possibly inaccurate due to large span drift  
 + Values assumed constant from those measured 1/5/82  
 † Calculated using the derived equation for kerosene as no CO data was available.

A similar form of this equation was used to adjust data obtained by the Electric Power Research Institute in studies they have done on synthetic fuels (16, 17, 18, 19). The equation they appear to have used raises the pressure ratio to a power of 1.5. I was unable to verify if this was a misprint in the article. In a conversation with Mr. Cohn of the EPRI it was indicated that this equation should not have been used for high Fuel-Bound Nitrogen fuels. The assumptions made in its derivation do not hold true when large amounts of  $\text{NO}_x$  from Fuel-Bound Nitrogen (FBN) are present.

Reference 16 states on Pg 4:

"The validity of this equation under water injection conditions is only partially established for low FBN fuels and not yet established for high FBN fuels".

In spite of these statements, all their data appears to have been adjusted using this type of equation. It was therefore decided to use the above equation to adjust all our data and thereby conform to their procedure. The pressure ratio was raised to the  $1/2$  power because it was felt that their use of 1.5 was a typographical error.

These adjusted values are in Table I in the column on the third from the right. The adjustment turned out to be minor, with a maximum change of -2 ppmv.

The actual combustor inlet conditions were determined from the ambient dry bulb temperatures and from the compressor outlet pressure. The compressor outlet temperature was calculated using air tables, and by assuming a compressor efficiency of 80%. The deriviations

leading to these values are given in Appendix 7. The actual inlet temperature was probably within  $10^{\circ}\text{F}$  of this value.

The carbon dioxide measurements were load dependent and remained fairly constant from fuel to fuel. There was some slight variation but this was well within our expected level of accuracy. The fuel composition did not effect these measurements. Upon checking the variation in carbon content of the three fuels used, it was found that the weight percent of carbon in the three fuels were within 1% of each other (see Appendix 8). The carbon dioxide levels would therefore not be expected to change.

The carbon monoxide was measured by reagent tube during the tests conducted on January 5, 1982. Because there was virtually no change in the carbon content of our fuel, or much change in our measured flame temperature, it was reasonable to expect little change in our CO output. We therefore made the assumption of identical CO values for the other runs at the same loads.

The measured combustor flame temperature was essentially constant for all our tested fuels, varying only with load. This might be expected as our turbine would control the fuel input to give a similar energy output for the loads, regardless of the fuel. This would result in similar combustion temperatures for similar fuels.

The value calculated as the combustion chamber temperature was the adiabatic flame temperature for the calculated air fuel ratio.

This temperature was found to be less than the measured value. This was unexpected as the energy consumed by dissociation reactions

in actual flames makes the adiabatic flame temperature (which does not take these into account) higher than the actual value.

In this case the discrepancy was probably due to incomplete mixing of the incoming air and the fuel at the point of measurement. The thermocouple was placed through the last set of air inlet holes in the combustor (see Figure 2). Final mixing of the products of combustion would then occur downstream of these holes.

Another factor supporting this assumption is that the discrepancy was greater at higher loads. At higher loads the fuel flow rate through the combustor was higher, which would cause the combustion zone to lengthen and come closer to the thermocouple. Also, the increased velocity of the combustion gases would move complete mixing further downstream.

In short, the adiabatic flame temperature under these circumstances would include dilution air in the calculations that did not actually take part in the combustion process.

In spite of these difficulties the adiabatic flame temperature is valuable as a general indicator of combustion conditions. It is a standard calculatable variable which is not prone to the variables that effect other methods of temperature measurement. It can be made much more accurate if the air fuel ratios are known for localized areas. Other methods of measurement such as thermocouples or infrared spectrometry are subject to interference by radiation from the flame zone and from the walls. In light of these variables our flame temperatures should be taken as indicators of trends rather than as absolute

Appendix 12 for the derivation and data for the adiabatic flame temperature.

In order for the adiabatic flame temperature calculations to be made, it was necessary that the air fuel ratio be determined. This was done three ways, by direct measurement, by assuming complete combustion and using chemical balances and  $\text{CO}_2$  measurements, and by the procedure recommended by the Society of Automotive Engineer's Aerospace Section. The latter was considered the most accurate and was used in almost all further calculations. It was necessary to use the second method for some points where carbon monoxide measurements were not available. The direct measurement method was used as a comparison.

For the direct measurement calculation it was necessary to modify the fuel density measurements to fit ambient conditions, (see Appendix 9) the calculations for the first two methods are given in Appendix 10.

The Society of Automotive Engineers, SAE ARP1256 method, gives the fuel air ratio by carbon balance as:<sup>20</sup>

$$F/A = \frac{(\% \text{ CO vol.}) + (\% \text{ CO}_2 \text{ vol.}) + (\% \text{ HC by' 81. as carbon})}{207 - 2*\text{CO}\% - \% \text{ CO}_2}$$

For the purpose of our test, the quantity of unburned hydrocarbons was so small as to consider it negligible.

In order to better comprehend the data, plots of  $\text{NO}_x$  against different variables were made;  $\text{NO}_x$  vs. measured flame temperature,  $\text{NO}_x$  vs. adiabatic flame temperature,  $\text{NO}_x$  vs. air fuel ratio and theoretical air, and  $\text{NO}_x$  vs. fuel bound nitrogen, at constant adiabatic flame temperature.

The plot of adjusted  $\text{NO}_x$  vs. measured flame temperature is shown in Figure 14. The points are fit very well by a linear approximation. A linear least squares fit of the results are shown in Table II.

TABLE II

Adjusted  $\text{NO}_x$  vs. Measured Flame Temperature

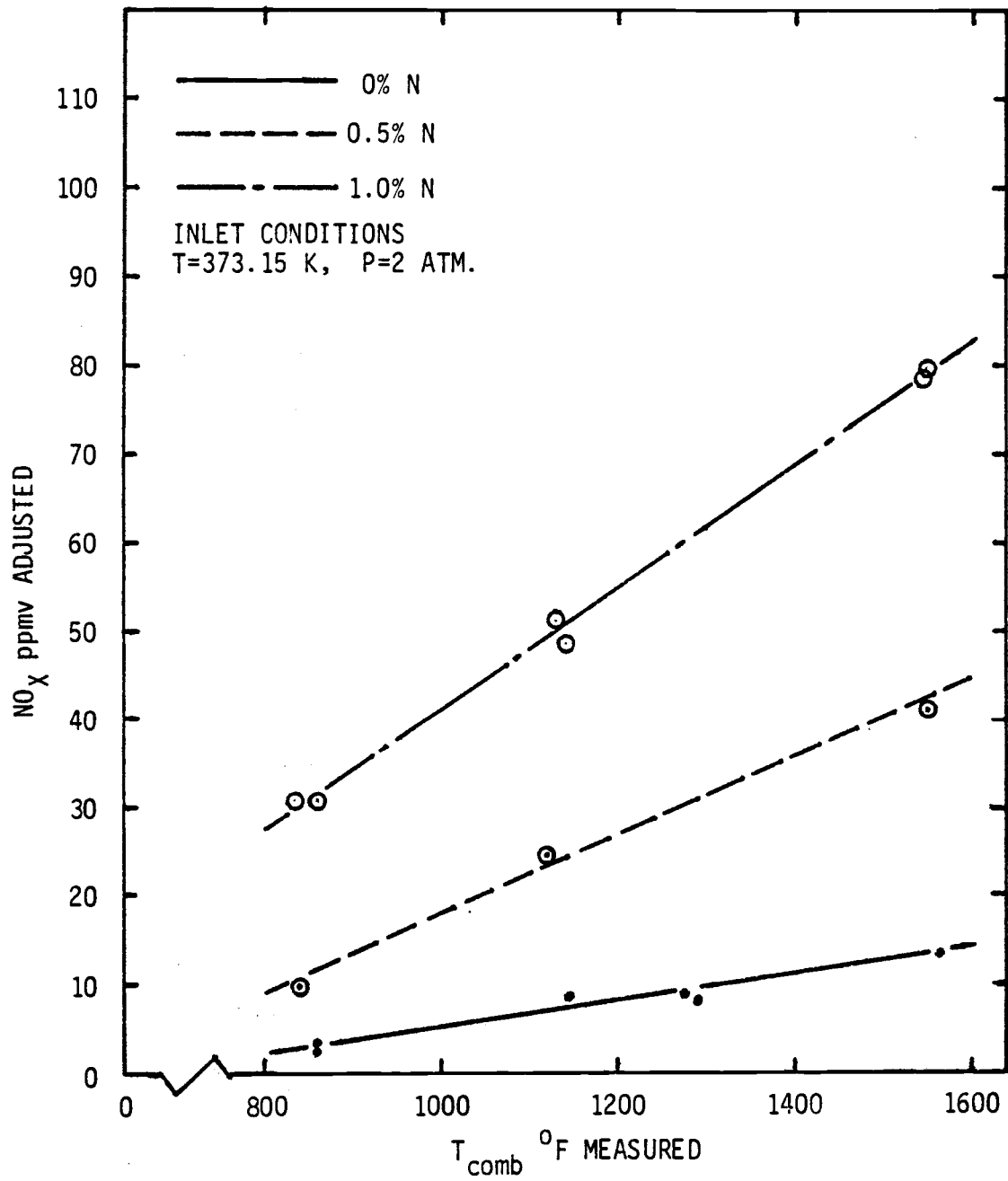
%N	$\text{NO}_x =$	$r^2$
0.0	- 9.134+0.0144 Tm	.955
0.5	-25.983+0.0437 Tm	.994
1.0	-26.917+0.0680 Tm	.996

As expected, the rate of production of  $\text{NO}_x$  increases with increased fuel bound nitrogen.

A comparison of this plot with those produced by the Electric Power Research Institute on subscale combustors<sup>21</sup> shows that these results are quite similar to theirs. Both tests produce straight line plots of  $\text{NO}_x$  vs. temperature. Figures 15 through 18 are a sample of some of their results. These tests were taking substitute fuels with similar characteristics to the actual synthetic fuels and comparing emissions.

An analysis of their results shows that they arrived at higher slopes than we did for similar nitrogen content fuels. There are a number of probable reasons for this. First of all, there are differences in the fuels' chemical composition, second their temperature measurement system was set up differently, and third, their inlet conditions were substantially different.

FIGURE 14  
ADJUSTED  $\text{NO}_x$  VS. MEASURED FLAME TEMPERATURE



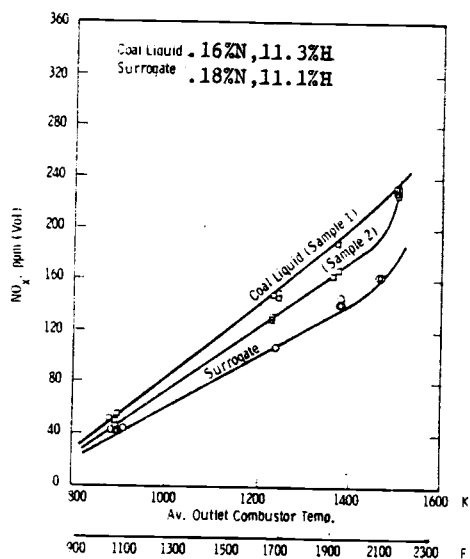


Figure 15 NO<sub>x</sub> emissions for H-coal (ATM-OVHD) 366-533 K and its surrogate

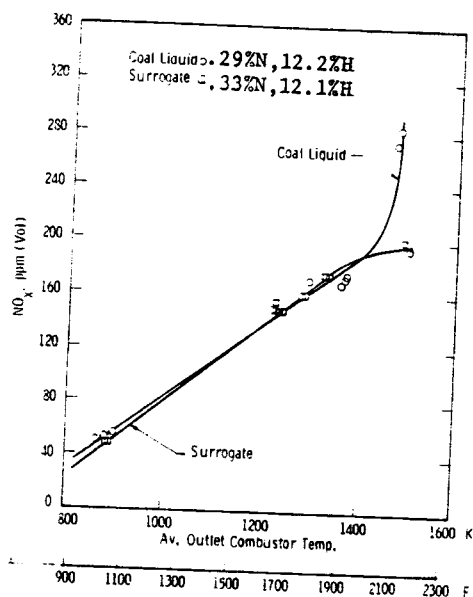


Figure 16 NO<sub>x</sub> emissions for SRC light organic, and its surrogate.

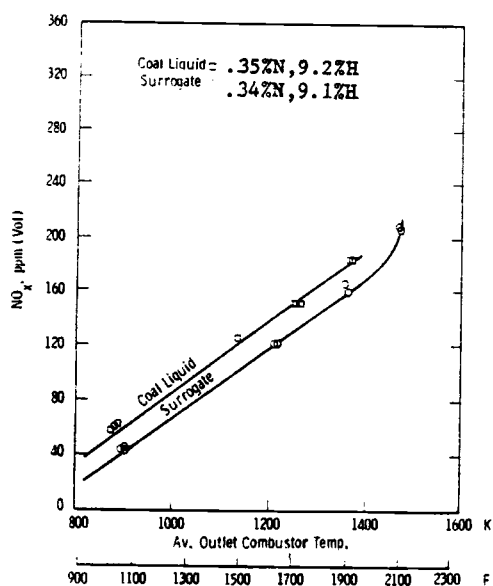


Figure 17 NO<sub>x</sub> emissions for SRC wash solvent and its surrogate

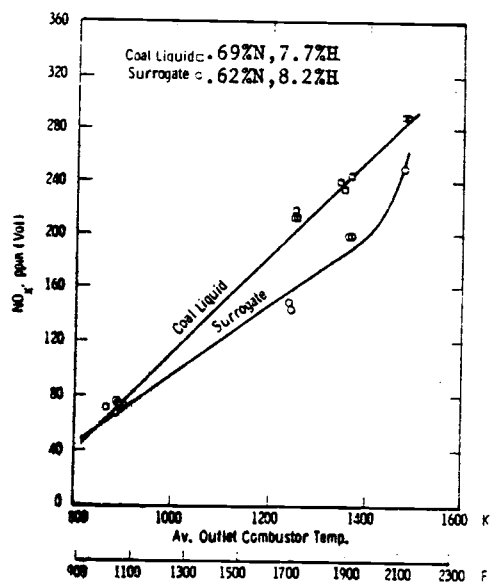


Figure 18 NO<sub>x</sub> emissions for SRC recycle solvent and its surrogate

They discovered during their testing that minor variations in chemical composition caused differences in emissions from small scale combustors. As an example, all of the surrogate fuels in Figures 15 through 18 had practically the same nitrogen, hydrogen, and aromaticity contents as the coal derived liquids that they were trying to imitate. It was found that small variations in nitrogen, oxygen and sulphur content can cause significant differences in  $\text{NO}_x$  emissions.<sup>22</sup> It was therefore quite likely that there would be some differences between their results and this test.

Their temperature measurement was done at an inverted hat mixer at the outlet to their combustor. At that point all their dilution and combustion air had been added and mixed. Even so, the lowest temperature for which they took readings appears to be around 1050°F. This is comparable to our half load condition in the combustion chamber itself. Their second lowest measurement was around 1700°F, higher than any of our temperatures.

Since these exhaust temperatures are so much higher than our internal combustor temperatures, it is probable that they had combustion chamber temperatures much higher than those in this study.

Further evidence to support this conclusion was gained when we noted that their combustor inlet temperatures and pressures were much higher than in this study. Their inlet conditions were 4 atm and 600°F, while this turbine had inlet conditions of around 2 atm and 215°F. These factors would greatly effect the combustion conditions.

It therefore was probable that our temperatures in the combustor were lower than their values.

It is interesting to note that extrapolation of most of the curves in Figure 15 through 18 will give zero values for  $\text{NO}_x$  at outlet temperatures of 500-800°F. As we are getting significant values for  $\text{NO}_x$  in this range (even with lower inlet conditions), there would appear to be a slope change in the data.

Another study by the EPRI by Singh et al.<sup>23</sup> confirms this. Unfortunately this paper in its entirety was not available. However, the team members in Part Two of the study, when explaining their choice of an exponential curve fit for their large scale combustor data state:

This equation form provides a close approximation for the straight line segments that are believed to represent the formation of  $\text{NO}_x$  combustors as discussed under subscale test results in Part I of this paper. The special fuel tests consisted of only four or five points for only three fuels so that characterization by straight line segments was not practical.<sup>24</sup>

It would seem likely that a number of production rates exist that vary over combustion conditions, and by being in a lower temperature range our production rate is therefore lower.

Figure 19 shows the results of a plot of  $\text{NO}_x$  vs. adiabatic flame temperature. This was also subject to linear regression analysis. The results of that analysis are given in Table III.

The slopes of the equations are slightly higher for this plot than against measured temperatures. This would indicate a higher rate of production of  $\text{NO}_x$  against changes in adiabatic flame conditions.

FIGURE 19

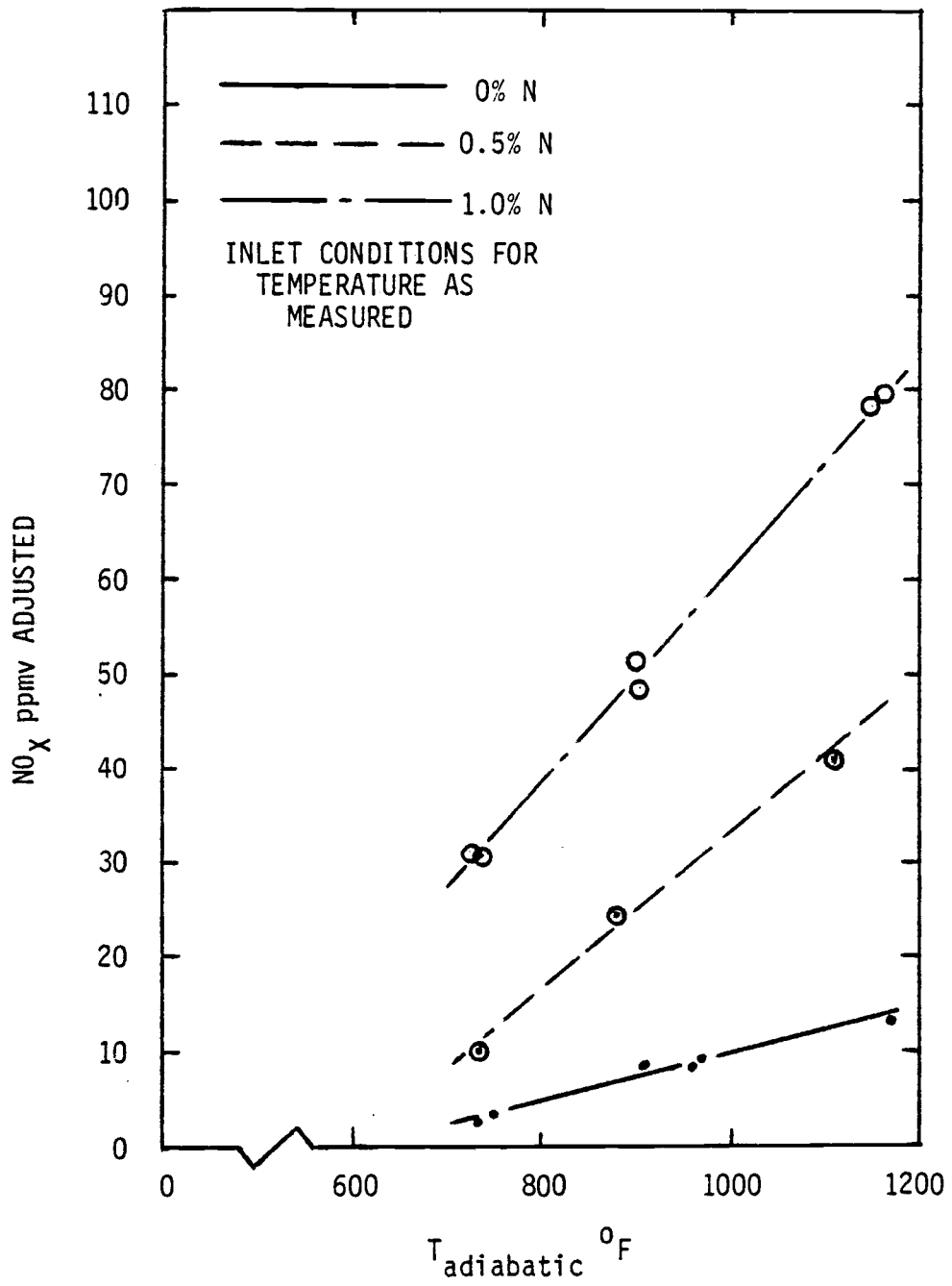
ADJUSTED  $\text{NO}_x$  VS ADIABATIC FLAME TEMPERATURE

TABLE III

Adjusted  $\text{NO}_x$  vs. Adiabatic Flame Temperature

%N	$\text{NO}_x =$	$r^2$
0.0	$-14.746 + 0.0245 T_{\text{adia}}$	.974
0.5	$-49.209 + 0.0819 T_{\text{adia}}$	.992
1.0	$-52.683 + 0.1139 T_{\text{adia}}$	.996

Even though the adiabatic flame temperature does not accurately reflect true combustion flame conditions in a gas turbine combustor, it does offer a standard against which other combustors, with similar overall energy outputs, can be compared.

The adjusted  $\text{NO}_x$  values were plotted against the air fuel ratio and theoretical air in Figure 20. These values, too, could be accurately fit to a linear approximation shown in Table IV.

TABLE IV

Adjusted  $\text{NO}_x$  vs. Air/Fuel Ratio and Theoretical Air

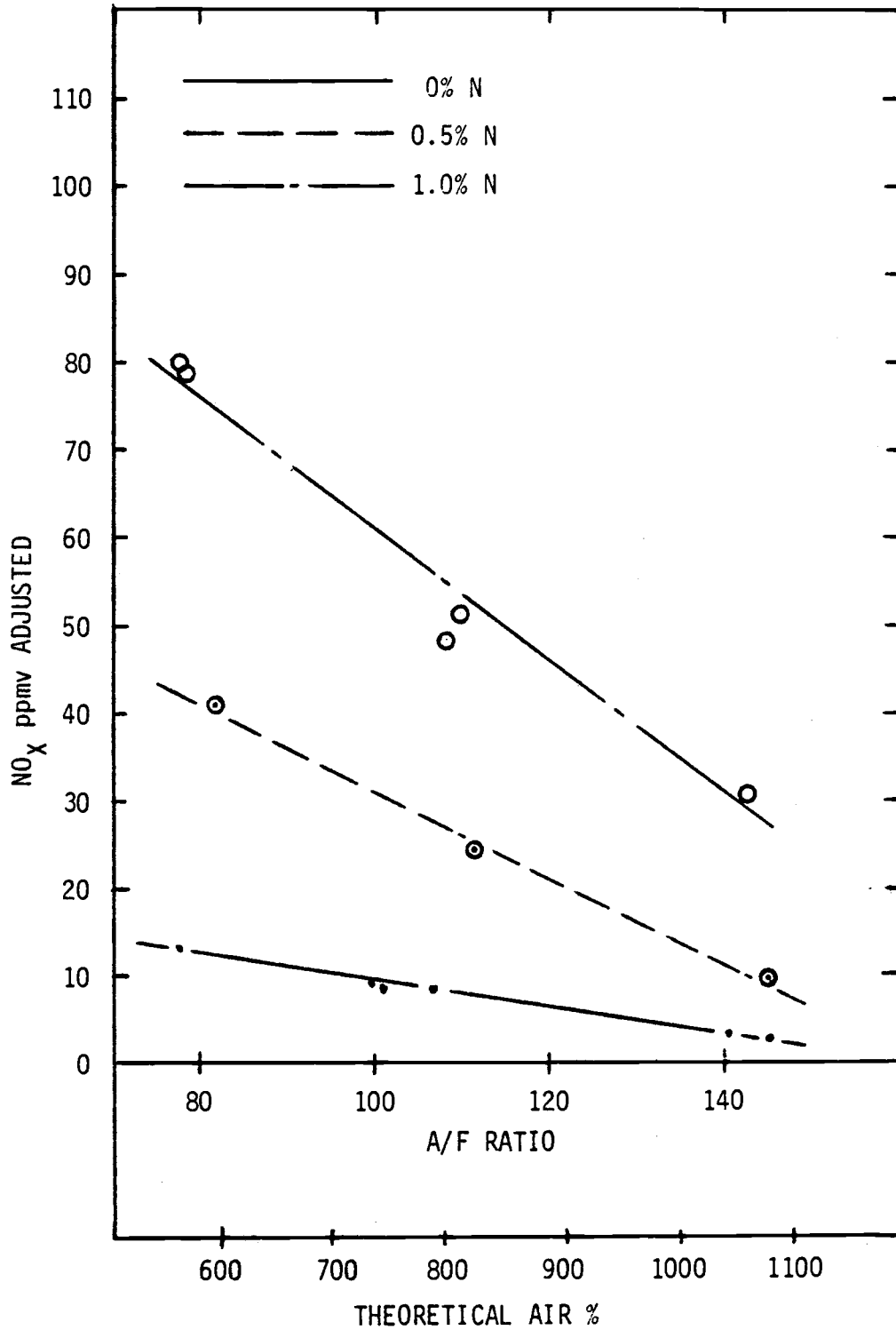
Linear Regression

%N	$\text{NO}_x =$	$r^2$
0.0	$24.711 - 0.1525 A/F$	.970
0.5	$80.530 - 0.4903 A/F$	.994
1.0	$135.259 - 0.7444 A/F$	.976

FIGURE 20

38

ADJUSTED  $\text{NO}_x$  VS AIR/FUEL RATIO  
AND  
THEORETICAL AIR



This shows a similar trend as the previous two plots. In this case, the  $\text{NO}_x$  values decrease linearly with increasing air fuel ratios. This would be anticipated as an increase in the air fuel ratio causes a corresponding decrease in the combustion temperature.

Perhaps the most interesting result of this study was the plot of  $\text{NO}_x$  against fuel bound nitrogen in Figure 21. These data were taken from Figure 19,  $\text{NO}_x$  vs Adiabatic Flame Temperatures, for constant temperatures. The temperatures chosen were those calculated at the average air fuel ratio for each load setting.

The plot of  $\text{NO}_x$  vs Adiabatic Flame Temperature was chosen so that an individual could roughly predict an  $\text{NO}_x$  value for a given fuel, air fuel ratio and combustor inlet condition. All of these contribute to the flame temperature.

The data points used are given in Table V. A number of types of curves were estimated for these data and the results are given in Table VI.

As can be seen from the plot and the regression coefficients in Table VI, the best fit equation for the lower temperature curve is an exponential fit. The best fit for the high temperature data, on the other hand, is a linear plot.

The conclusion that was drawn from this was that at higher temperatures the production rate was less dependent on fuel bound nitrogen content than at lower temperatures. The production rate was

FIGURE 21  
ADJUSTED  $\text{NO}_x$  VS FUEL BOUND NITROGEN  
AT  $T_{\text{adiabatic}}$

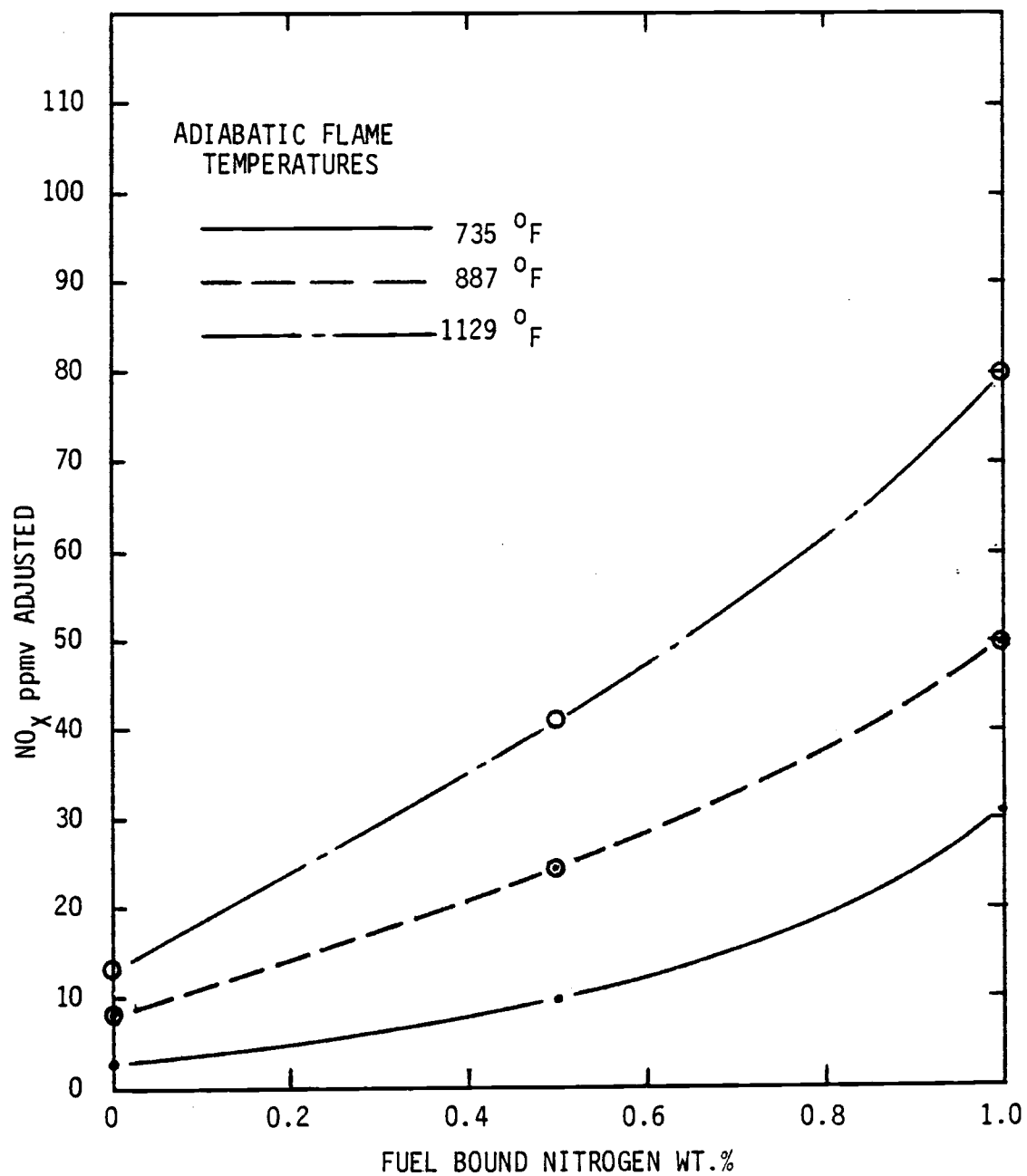


TABLE V

NO<sub>x</sub> vs Fuel Bound NitrogenNO<sub>x</sub> ppmv

T adiabatic FBN	0.0	0.5	1.0
735°F	3.0	10.8	30.4
887°F	6.8	23.2	48.0
1129°F	12.7	43.2	76.0

TABLE VI

NO<sub>x</sub> vs. Fuel Bound Nitrogen Least Squares Curve Fits

T adiabatic	Power Curve Fit	r <sup>2</sup>	Exponential Curve Fit	r <sup>2</sup>
735°F	20.44*FBN <sup>(.28)</sup>	.87	3.126e <sup>2.316FBN</sup>	.996
887°F	35.98*FBN <sup>(.18)</sup>	.91	7.391e <sup>1.954FBN</sup>	.979
1129°F	61.37*FBN <sup>(.17)</sup>	.94	14.175e <sup>1.789FBN</sup>	.957

T adiabatic	Linear Curve Fit	r <sup>2</sup>
735°F	1.033 + 27.4 FBN	.941
887°F	5.4 + 41.2 FBN	.986
1129°F	12.32 + 63.3 FBN	1.000

essentially constant (constant slope), while the production rate for lower temperatures increased (increasing slope).

One possible explanation for this is that at higher loads there were higher amounts of thermal  $\text{NO}_x$  present, which would lower the relative contribution of the fuel bound nitrogen to overall  $\text{NO}_x$ . At higher fuel flow rates there may also be reduced primary air penetration to the center of the combustion zone. This might provide a sufficiently rich (oxygen starved) area to inhibit the formation of fuel bound nitrogen  $\text{NO}_x$ , slightly.

The overall production rate still increased with temperature, as can be seen from the linear approximations of the data. The production rate at constant temperature was higher for the high temperatures (a slope of 63.3) than for the lower temperature (a slope of 27.4).

These statements say nothing about the amount of conversion of fuel bound nitrogen to  $\text{NO}_x$ . This is concerned only with the total production of  $\text{NO}_x$ , both thermal and fuel bound nitrogen  $\text{NO}_x$ , combined.

It was not possible to calculate the percent conversion of fuel bound nitrogen to  $\text{NO}_x$  due to the inaccuracy of some of the experimental methods. Recent research by Vermes, Toof, and Cohn<sup>25</sup> indicates that the production of thermal  $\text{NO}_x$  is not constant, which is what the percent conversion method assumes. Their studies indicate

that the presence of  $\text{NO}_x$  from fuel bound nitrogen will inhibit the formation of thermal  $\text{NO}_x$ . For this reason, there is much argument over the actual amount of FBN conversion and over the actual thermochemical balances involved. This is an argument well beyond my area of expertise.

## CONCLUSION

The results of this work are similar to that generated by other experimenters. We have measured  $\text{NO}_x$  values which are lower than the other studies; however, the lower values can be attributed to lower combustion temperatures, and to differences in fuels and inlet conditions.

The production rate of  $\text{NO}_x$  versus fuel bound nitrogen content was found to be less dependent on nitrogen content at higher temperatures than at lower values. The overall rate of  $\text{NO}_x$  production drop was found to be higher for the higher temperatures.

A plot of  $\text{NO}_x$  versus fuel bound nitrogen at constant adiabatic flame temperatures was made. This can be used to predict  $\text{NO}_x$  values for other nitrogen content fuels of the same fuel type.

Great care should be used in applying these results to large scale turbines or in using the above plot to predict  $\text{NO}_x$  values for machines with significantly different pressure ratios. Studies conducted on both large and small scale combustors by the Electric Power Research Institute, indicate that the results from small scale studies do not always accurately predict full scale results.<sup>26</sup>

## REFERENCES

1. Pg 2 EPA Research Summary Controlling Nitrogen Oxides, EPA-600/8-80-004.
2. Dr. Richard Boubel, Class Lecture ME 490, Oregon State University, 10/6/80.
3. Pg 5 EPA Pamphlet, "Acid Rain", Publication number EPA-600/9-79-036, July 1980.
4. Ibid., p. 16.
5. Pg 85, "Researchers Study effects of Acid Rain on Marine Life", Mechanical Engineering, November 1981.
6. Shale Oil - The Answer to the Jet Fuel Availability Question. L. C. Angello, Wright Patterson Air Force Base, 1978, SAE Publication 78/027.
7. Glassman, Irvin; "Combustion", Academic Press, San Francisco, 1977, pp. 221-225.
8. Fenimore, C. P. (1971), Int. Symp. Combust. 13th, p. 373. Combustion Inst. Pittsburg, Penn.
9. Operations Manual, Scott Chemiluminescence Analyzer, Model 325. Environmental Tectonics Corporation, Southampton, PA, pp. 4-8.
10. Campbell, N. T.; Beres, G.A.; Blasko, T. J.; and Groth, R. H., "Problems in the Measurement of Nitrogen in Gas Turbine Engine Exhaust", Presentation to the 74th Annual Meeting of the Air Pollution Control Association. Philadelphia, PA 1981, pp. 8, 14.
11. Beckman 215A Infrared Analyzer instructions B1635-2, Beckman Instruments, Inc., Fullerton, CA, July 1969, pg. ii.
12. Technical Publications Section, "Easterline Angus"; Operating Instructions for Speed Servo R II Strip Chart Recorders", M70A1, 1M572, 1972, p. 3.
13. Personal communication with Richard Wielesic at the University of Oregon Chemistry Labs, 9/17/81.
14. Lewis, G. D. Prediction of NO<sub>x</sub> Emissions, paper presented to the 1981 ASME Gas Turbine Conference and Products Show. Paper No. 81-GT-119.

15. EPA Proposed Revisions to Gaseous Emissions Rules for Aircraft and Aircraft Engines, 43 FR 12615, March 24, 1978, 40 CFR Part 87.21 d(iii)b.
16. P. R. Mulik, P. P. Singh, A. Cohn; "Effect of water injection for NO<sub>x</sub> Reduction with Synthetic Liquid Fuels Containing High Fuel-Bound Nitrogen in a Gas-Turbine Combustor. Presented to the 1981 ASME Gas Turbine Conference and Products Show, ASME Paper #81-GT-51.
17. P. R. Singh, E. R. Bazarian, P. R. Mulik, G. W. Bauserman, A. Cohn, T. R. Stein; "Comparative Testing of Petroleum Surrogate Fuels with Coal-Derived Liquids in a Combustion Turbine Burner." Presented to the 1980 ASME Gas Turbine Conference and Products Show, ASME Paper No. 80-GT-64.
18. P. P. Sing, et al., "Combustion Effects of Coal Liquid and Other Synthetic Fuels in Gas Turbine Combustors - Part I: Fuels Used and Subscale Combustion Results". Presented to the 1980 Gas Turbine Conference and Products Show, ASME Paper No. 80-GT-67.
19. G. W. Bauserman, C. J. Spengler, A. Cohn; "Combustion Effects of Coal Liquid and Other Synthetic Fuels in Gas Turbine Combustors - Part II: Full Scale Combustor and Corrosion Tests". Presented to the 1980 Gas Turbine Conference and Products Show, ASME Paper No. 80-GT-68.
20. Society of Automotive Engineers Aerospace Recommended Practice, "Procedure for the Continuous Sampling and Measurement of Gaseous Emissions from Aircraft Turbine Engines", October 1, 1971 SAE, APR 1256.
21. Op Cit, 80-GT-64, pp. 5-6.
22. Ibid, p. 6.
23. Op Cit, Singh, 80-GT-67.
24. 80-GT-68, p. 3.
25. Vermes, G., Toof, J. L., Cohn, A.; "The Modeling of NO<sub>x</sub> Generation from Coal Derived Liquids in Combustion Turbines"; Paper 79-JP GC-GT-4, presented at the Joint ASME/IEEE/ASCE Power Generation Conference, Charlotte, N.C., Oct. 8-10, 1974.
26. Op Cit, Bauserman, 80-GT-68, p. 10.
27. Skrotzski and Vopat, "Power Station Engineering and Economy", McGraw-Hill 1960, pp. 724-725.

28. Chilton and Perry, Chemical Engineers Handbook, pp. 9-11.
29. Hodgman, Charles, Handbook of Chemistry and Physics, 21st Edition, 1936-37, p. 1199.
30. F. W. Dwyer Mfg. Co., Inc., Michigan City, Ind., "Pitot Tube Bulletin No. H 11".
31. M. Popovich and C. Hering, "Fuels and Lubricants", John Wiley and Sons, Dec. 1973, p. 15.
32. Ibid., p. 16.
33. Wark, Thermodynamics, 3rd edition, McGraw-Hill Book Co., 1977, San Francisco, pp. 609-614.

## BIBLIOGRAPHY

- Angello, L. C.; "Shale Oil - The Answer to the Jet Fuel Availability Question"; SAE Publication 781027, Wright Patterson Air Force Base, 1978.
- Bauserman, G. W., et al.; "Combustion Effects of Coal Liquid and Synthetic Fuels in Gas Turbine Combustors - Part II: Full Scale Combustors and Corrosion Tests"; ASME Publication No. 80-GT-68, March 1980.
- Bittker, D. A. et al.; "Effect of Fuel Bound Nitrogen and Hydrogen on Emissions in Hydrocarbon Combustion". ASME Publication 81-GT-63, March 1981.
- Beckman 215A Infrared Analyzer Instructions 81635-C; Beckman Instruments, Inc., Fullerton, CA July 1969.
- Campbell, N. T.; "Gas Turbine Engine Emissions Measurement Technology - An Overview"; ASME Publication No. 80-GT-86, March 1980.
- Campbell, N. T., Beres, G. A. et al.; "Problems in the Measurement of Nitrogen in Gas Turbine Engine Exhaust"; Presentation to the 74th Annual Meeting of the Air Pollution Control Association, Philadelphia, PA, 1981.
- Chilton and Perry, Chemical Engineers Handbook.
- Dwyer Manufacturing Co., Inc.; "Pitot Tube Bulletin No. H 11", Michigan City, IN.
- E.P.A. Pamphlet; "Acid Rain", Publication number EPA-600/9-79-036, July 1980.
- EPA Revisions; "E.P.A. Proposed Revisions to Gaseous Emissions, Rules for Aircraft and Aircraft Engines". 43 FR 12615, 40 CFR Part 87.21, March 24, 1978.
- EPA Research Summary; "Controlling Nitrogen Oxides". Report No. EPA-600/8-80-004.
- Easterline Angus, Technical Publications Section; "Operating Instructions for Speed Servo<sup>R</sup> II Strip Chart Recorders" M70 A1, 1M572, 1972.

- Federal Register Vol. 38; "Control of Air Pollution from Aircraft and Aircraft Engines". No. 136, Part II, July 17, 1973.
- Fenimore, C. P.; International Symposium on Combustion 13th., Combustion Institute, Pittsburgh, PA, 1971.
- Gaydon, A. G.; Wolfhard, H. G.; "Flames, Their Structure, Radiation and Temperature"; Chapman and Hill, London, 1979.
- Glassman, Irvine; "Combustion"; Academic Press; San Francisco, 1977.
- Hodgman, Charles; "Handbook of Chemistry and Physics, 21st Edition 1936-1937", Chemical Rubber Publishing Co., Cleveland, OH.
- Jackson, T. A.; "The Evaluation of Fuel Property Effects on Air Force Gas Turbine Engines - Program Genesis". ASME 81-GT-1, March 1981.
- JANAF, Thermochemical Tables, The Dow Chemical Co., Thermal Laboratory, Midland, MI
- Lewis, G. D.; "Prediction of NO<sub>x</sub> Emissions", ASME Publication 81-GT-119; March, 1981.
- Mechanical Engineering Magazine; "Researchers Study Effects of Acid Rain on Marine Life", Nov. 1981.
- Mulik, P. R., et al.; "Effect of Water Injection for NO<sub>x</sub> Reduction with Synthetic Liquid Fuels Containing High Fuel Bound Nitrogen in a Gas Turbine Combustor". ASME Publication 81-GT-51, March 1981.
- Popovich, M., and Hering, C; "Fuels and Lubricants", John Wiley and Sons, Dec. 1973.
- Society of Automotive Engineers Recommended Practice 1256, "Procedure for the Continuous Sampling and Measurement of Gaseous Emissions from Aircraft Turbine Engines". October 1971.
- Scott, H. A., Jr.; "The Implications of Alternative Aviation Fuels on Airbase Air Quality"; Air Force Engineering and Services Center, Publication number ESL-TR-80-38; August 1980.
- Scott Chemiluminescence Analyzer, Model 325, Operations Manual, Environmental Tectonics Corp., Southampton, PA
- Singh, P. P.; "Comparative Testing of Petroleum Surrogate Fuels with Coal Derived Liquids in a Combustion Turbine Burner." ASME Publication No. 80-GT-64, March 1980.

- Singh, P. P. et al.; "Combustion Effects of Coal Liquid and other Synthetic Fuels in Gas Turbine Combustors - Part I: Fuels Used and Subscale Combustion Results". ASME Publication No. 80-GT-67.
- Skrotzski and Vopat; "Power Station Engineering and Economy", McGraw-Hill, 1960.
- Vermes, G., Toof, J. L., Cohn, A.; "The Modeling of NO<sub>x</sub> Generation from Coal Derived Liquids in Combustion Turbines". Presented at the Joint ASME/IEEE/ASCE Power Generation Conference, Charlotte, N.C.; Oct. 8-10, 1979, Paper No. 79-JPGC-GT-4.
- Wark, "Thermodynamics, 3rd edition", McGraw-Hill Book Co., San Francisco, CA, 1977.
- White, D. J.; "Low NO<sub>x</sub> Combustion Systems for Burning Heavy Residual Fuels and High Fuel-bound Nitrogen Fuels", ASME Publication No. 81-GT-109, March 1981.
- Williams, Alan; "Combustion of Sprays of Liquid Fuels"; Paul Elek (Scientific Books) Ltd., London, 1976.
- Zeldovich, A.; "The Oxidation of Nitrogen in Combustion and Explosives"; Acta Physiocochemica U.R.S.S., Vol. 21, Nov. 4, 1946.

## APPENDICES

## APPENDIX 1

Test of Scott NO<sub>x</sub> Analyzer Accuracy

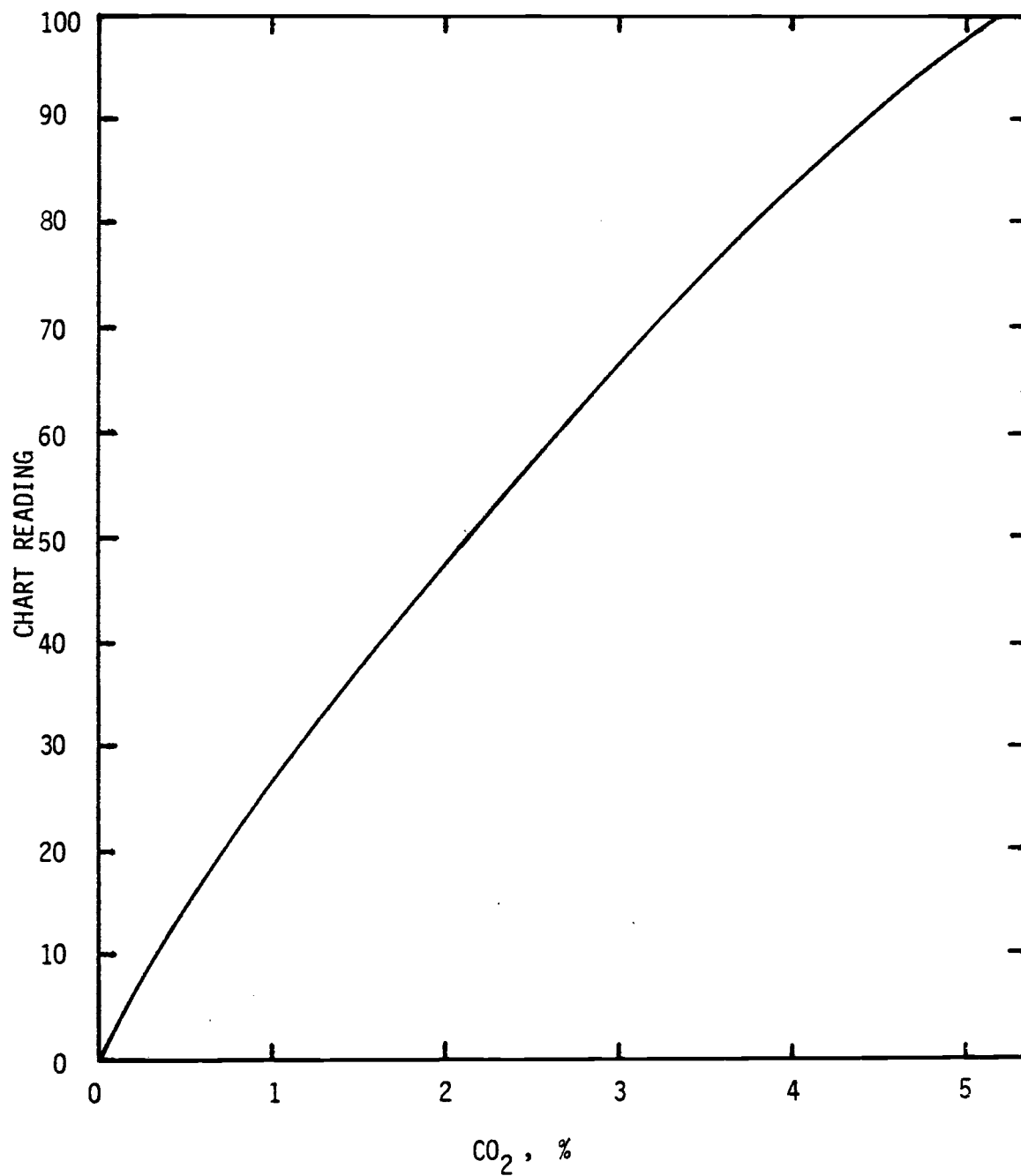
1/2/82 Calibrated on 45 ppmv span gas on 100 ppmv range

Zero pot: initial-2.458 final-2.32  $\Delta\%$  scale = 4.3%

Gain pot: initial-4.179 final-4.08  $\Delta\%$  scale = 1.0%

Span Gas ppmv	Instrument Range			Error %
	100 ppmv	250 ppmv	10,000 ppmv	
45	45			0
95	97-100			+2-+5
		92.5-95		-1. -0.
2460			2650	+1.9

APPENDIX 2  
BECKMAN NDIR CO<sub>2</sub>  
CALIBRATION 2-27-81



## APPENDIX 3

## Calculation of Required Additive Volume for a Given Weight Percent of Mixed Fuel

$$12 \quad 1. \quad \text{Wt \%}_1 \text{ Mix} = \frac{\text{Wt \%}_1 \text{ Total}}{\text{Wt \%}_1 \text{ Total}} = \frac{\text{Wt \% 1} * (V_1 * \rho_1) + \text{Wt \% 2} * (V_2 * \rho_2)}{(V_1 * \rho_1) + (V_2 * \rho_2)}$$

where Wt %<sub>1</sub> Mix - Weight percent of the desired element in the final mixture

Wt Total - Total weight of the final mixture

Wt % 1 - Weight percent of the desired element in the additive

V<sub>1</sub> - Volume of the additive in the final mix

ρ<sub>1</sub> - Density of the additive

Wt % 2 - Weight percent of the desired element in the base fuel

V<sub>2</sub> - Volume of the base fuel in the final mix

ρ<sub>2</sub> - Density of the base fuel

$$2. \quad \text{Volume total} = V_1 + V_2$$

$$= V_1 \left[ 1 + \left( \frac{V_2}{V_1} \right) \right]$$

$$3. \quad \text{Taking eq. 1 and solving for } \frac{V_2}{V_1}$$

$$\text{Wt \%}_1 \text{ mix} = \frac{(\text{Wt \% 1} * \rho_1) + (\text{Wt \% 2} * \left( \frac{V_2}{V_1} \right) * \rho_2)}{\rho_1 + \left( \left( \frac{V_2}{V_1} \right) * \rho_2 \right)}$$

$$\frac{(\text{Wt \%}_1 * \rho_1) + (\text{Wt \% 2} * \left( \frac{V_2}{V_1} \right) * \rho_2)}{\text{Wt \%}_1 \text{ Mix}} = \rho_1 + \left[ \left( \frac{V_2}{V_1} \right) * \rho_2 \right]$$

$$\frac{\text{Wt \% 1} * \rho_1}{\text{Wt \%}_1 \text{ mix}} + \frac{\text{Wt \% 2} * \left( \frac{V_2}{V_1} \right) * \rho_2}{\text{Wt \%}_1 \text{ mix}} = \rho_1 + \left[ \left( \frac{V_2}{V_1} \right) * \rho_2 \right]$$

$$\frac{\text{Wt \% 1} * \rho_1}{\text{Wt \%}_1 \text{ mix}} = \rho_1 + \left[ \left( \frac{V_2}{V_1} \right) * \rho_2 \right] - \frac{\text{Wt \% 2} * \left[ \left( \frac{V_2}{V_1} \right) * \rho_2 \right]}{\text{Wt \%}_1 \text{ mix}}$$

$$\frac{\text{Wt \% 1} * \rho_1}{\text{Wt \%}_1 \text{ mix}} - \rho_1 = \left( \frac{V_2}{V_1} \right) * \rho_2 \left( 1 - \frac{\text{Wt \% 2}}{\text{Wt \%}_1 \text{ mix}} \right)$$

$$\begin{aligned} \frac{V_2}{V_1} &= \rho_1 * \left( \frac{\text{Wt \% 1}}{\text{Wt \% mix}} - 1 \right) * \left( \frac{1}{\rho_2 \left( 1 - \frac{\text{Wt \% 2}}{\text{Wt \% mix}} \right)} \right) \\ &= \left( \frac{\rho_1}{\rho_2} \right) * \left( \frac{\text{Wt \% 1}}{\text{Wt \% mix} \left( 1 - \frac{\text{Wt \% 2}}{\text{Wt \%}_1 \text{ mix}} \right)} - \frac{1}{\left( 1 - \frac{\text{Wt \% 2}}{\text{Wt \%}_1 \text{ mix}} \right)} \right) \end{aligned}$$

4. Solving eq. 2. for  $V_1$  (additive Volume)

$$V_1 = \frac{\text{Volume Total}}{1 + \frac{V_2}{V_1}}$$

5. Substituting 3. into 4.

$$V_1 = \frac{\text{Volume Total}}{1 + \left( \frac{\rho_1}{\rho_2} \right) * \left( \frac{\text{Wt \% 1}}{\text{Wt \%}_1 \text{ mix} \left( 1 - \frac{\text{Wt \% 2}}{\text{Wt \%}_1 \text{ mix}} \right)} - \frac{1}{\left( 1 - \frac{\text{Wt \% 2}}{\text{Wt \%}_1 \text{ mix}} \right)} \right)}$$

6. and simplifying

$$13 \quad V_1 = \frac{\text{Volume Total}}{1 + \left( \frac{\rho_1}{\rho_2} \right) * \left( \frac{\text{Wt \% 1} - \text{Wt \%}_1 \text{ mix}}{\text{Wt \%}_1 \text{ mix} \left( 1 - \frac{\text{Wt \% 2}}{\text{Wt \%}_1 \text{ mix}} \right)} \right)}$$

A computer program employing this equation and a printout of the results for the nitrogen contents desired in this study follow.

## LIST

```
10 REM THIS PROGRAM CALCULATES THE VOLUME OF ADDATIVE REQUIRED
20 REM FOR A GIVEN MIX CONCENTRATION OF THE DESIRED ELEMENT
30 ! CHR$(27),CHR$(64)
40 ! CHR$(12)
50 PRINT " INPUT THE WIEGHT PERCENT OF THE DESIRED ELEMENT IN YOUR "
60 PRINT "ADDATIVE AND YOUR BASE FUEL.(IN DECIMAL FORM.)"
70 INPUT W1,W2
80 PRINT " "
90 PRINT " INPUT THE DENSITY OF THE ADDATIVE AND THE BASE FUEL."
100 INPUT D1,D2
110 !" "
120 PRINT " INPUT THE DESIRED WIEGHT PERCENT OF THE ELEMENT IN "
130 PRINT "THE MIX ,AND THE TOTAL AMOUNT OF MIX WANTED."
140 INPUT W,V1
150 B=(W1-W)/(W*(1-(W2/W)))
160 V2=V1/(1+(D1/D2)*B)
170 V3=V1-V2
175 !" "\ !" "
180 PRINT "ADD ",V2," ADDATIVE TO ",V3," BASE FUEL. "
185 PRINT "THE ADDATIVE TO BASE VOLUME RATIO IS ",V2/V3
190 END
READY
```

Mixes Used1.0% Nitrogen

INPUT THE WIEGHT PERCENT OF THE DESIRED ELEMENT IN YOUR  
ADDATIVE AND YOUR BASE FUEL.(IN DECIMAL FORM.)

T.1783,0.0

INPUT ERROR-RETYPE

T.1783,0.0

INPUT THE DENSITY OF THE ADDATIVE AND THE BASE FUEL.

T.9765,7934

INPUT THE DESIRED WIEGHT PERCENT OF THE ELEMENT IN  
THE MIX ,AND THE TOTAL AMOUNT OF MIX WANTED.

T.01,189 26.65

ADD 871.63315 ADDATIVE TO 16055.017 BASE FUEL.

THE ADDATIVE TO BASE FUEL VOLUME RATIO IS 4.8276507E-02

READY

RUN

0.5% Nitrogen

INPUT THE WIEGHT PERCENT OF THE DESIRED ELEMENT IN YOUR  
ADDATIVE AND YOUR BASE FUEL.(IN DECIMAL FORM.)

T.1783,0.0

INPUT THE DENSITY OF THE ADDATIVE AND THE BASE FUEL.

T.9765,7934

INPUT THE DESIRED WIEGHT PERCENT OF THE ELEMENT IN  
THE MIX ,AND THE TOTAL AMOUNT OF MIX WANTED.

T.003,18926.65

ADD 433.51286 ADDATIVE TO 18493.137 BASE FUEL.

THE ADDATIVE TO BASE FUEL VOLUME RATIO IS 2.3441824E-02

READY

## APPENDIX 4

## GAS TURBINE DATA SHEET

USAF Project - Laboratory Evaluation of Novel Particulate  
Control Concepts for Jet Engine Test Cells

Principal Investigator Prof. R. W. Boubel  
Oregon State University

Date \_\_\_\_\_ Time \_\_\_\_\_

Test Crew \_\_\_\_\_

Type of Control Device \_\_\_\_\_

Fuel: % Kerosene \_\_\_\_\_, % Toluene \_\_\_\_\_

Ambient Temperature, °F \_\_\_\_\_ Barometric Pressure, in. Hg \_\_\_\_\_

Fuel Flow: Seconds per 2000 cc \_\_\_\_\_, Pounds per hour \_\_\_\_\_

Fuel Pressure, psi \_\_\_\_\_ Compressor Outlet Pressure, psi \_\_\_\_\_

Turbine Load ( 0, 1/2, Full ), Kw \_\_\_\_\_

Exhaust: CO<sub>2</sub>, Reading \_\_\_\_\_, % \_\_\_\_\_ Opacity, % \_\_\_\_\_

Turbine Outlet Temperature, °F \_\_\_\_\_

NO<sub>x</sub>, Reading \_\_\_\_\_, % \_\_\_\_\_

Velocity Pressure ( 1 in. from top), in. H<sub>2</sub>O \_\_\_\_\_ Vel., fpm \_\_\_\_\_

Smoke Sample: Orifice Δp, in. H<sub>2</sub>O \_\_\_\_\_ Time, Sec. \_\_\_\_\_

Flow, cfh \_\_\_\_\_ Gas Volume, cubic feet \_\_\_\_\_

Sample Temperature, °F \_\_\_\_\_

Rw (Reflectance of clean filter) \_\_\_\_\_

Rs (Reflectance of Sample Spot) \_\_\_\_\_

Smoke Number \_\_\_\_\_

Maximum Duct Temperature, °F \_\_\_\_\_

Remarks Twb1- Tdb1- Twb2- Tdb2-

\_\_\_\_\_

\_\_\_\_\_

\_\_\_\_\_

## APPENDIX 5

## GAS TURBINE OPERATING PROCEDURE (modified 6/26/81)

## A. 2 hours before test

- 1) Place NOx Exhaust and Bypass out window
- 2) Turn on N<sub>2</sub> Cylinder and adjust to 10 psi
- 3) Turn on Power to CO<sub>2</sub> analyzer turnswitch to TUNE
- 4) Turn on Power to NOx analyzer and push the ZERO and CONV buttons on NOx system
- 5) Turn 3 way valve on CO<sub>2</sub> system to N<sub>2</sub> and adjust flow through CO<sub>2</sub> system to 800 cc/min
- 6) Adjust NOx analyzer to 5½ psi (sample valve) and 1½ SCFH flow rate

## B. Test procedure

- 1) Open test turbine exhaust duct damper
- 2) Ensure fuel supply in proper tanks (measuring burette filled)
- 3) Turn on fuel supply valves to turbine (four valves in all)
- 4) Connect battery (red to positive)
- 5) Turn on panel lights (if lights come on battery's are o.k.)
- 6) Turn on opacity monitor blower (plug in)
- 7) Turn on opacity monitor and recorder (adjust zero and span on both)
- 8) Turn on exhaust duct blower (switch is on column next to fuel tank)
- 9) Turn on electrical load cooling blower
- 10) Turn on Relative Humidity measuring device
- 11) Turn on CO<sub>2</sub>, NOx span and Air Tanks
- 12) Adjust CO<sub>2</sub> pressure to 5-6 psi and the NOx and Air Tanks to 10-15 psi
- 13) Turn on all Line Valves (following regulators)
- 14) With threeway valve in N<sub>2</sub> position adjust the CO<sub>2</sub> analyzer until the meter reads zero.
- 15) Adjust the CO<sub>2</sub> recorder to zero
- 16) Turn threeway valve to CO<sub>2</sub> adjust the instrument gain to get 100% on recorder
- 17) Recheck N<sub>2</sub>+CO<sub>2</sub> until consistant valves are obtained.
- 18) Turn on compressed air to sample delivery system (on wall near boiler)
- 19) Plug in sample delivery system (electrical)
- 20) Turn on Ambient and pump switches on sample delivery system panel
- 21) Turn threeway valve to sample and adjust CO<sub>2</sub> instrument flow to 800 cc/min
- 22) Press samp switch on NOx instrument (light should glow)
- 23) Adjust sample pressure to 5.5 psi
- 24) Adjust sample flow to 1.5SCFH bypass
- 25) Turn on OXY button and adjust air pressure to 5.5 psi
- 26) Turn on O<sub>2</sub> and NOx buttons
- 27) Zero adjust for NOx
  - a) Press Zero button, press 100 range switch
  - b) Zero instrument to slightly positive
  - c) Check recorder and adjust zero with span (screw driver) if needed
- 28) Span adjustment for NOx
  - a) Press Span button and 100 range scale
  - b) Adjust cylinder until sample pressure reads 5.5
  - c) Adjust gain to proper value on instrument
  - d) Check recorder for same value adjust with the zero if necessary

- 29) Recheck zero and span and adjust as needed to obtain consistent values
- 30) Make notation on chart of pot settings, date and run number
- 31) Press the Samp switch on the NOx instrument
- 32) Press the sample switch on the sample delivery system panel
- 33) Record, Tdbulb, Twb
- 34) Check turbine panel switches all off or open
- 35) Start turbine (RPM-100%, Volts-240, amps &KW-0)
- 36) Set load switch to position L<sub>1</sub> L<sub>3</sub> PH 3
- 37) Select 0, ½, or Full Load
- 38) Take all Data
- 39) Rerecord Tdbulb, Twb
- 40) Shut down turbine
- 41) Purge NOx and CO<sub>2</sub> instruments with N<sub>2</sub> or ambient Air
- 42) Recheck all calibrations and note changes on strip shrct
- 43) Purge sample line and cooling system by pushing the Shop Air and Trap drain buttons on sample transport system panel
- 44) Shut down all machinery and equipment in the reverse order of start up

## APPENDIX 6

NO<sub>x</sub> Values from Data Sheets  
(when more than one reading was taken)

Test 1/5/82 Load - 0

Fuel 0% N

	read	0	Δ
1)	5	1.5	3.5
2)	5.5	1.75	3.75
3)	4.5	1.0	3.5
4)	4	1.5	2.5

$$\bar{\Delta} = 3.2 \quad \sigma = .31$$

Test 1/5/82 Load - 6.25

Fuel 0% N

	read	0	Δ
1)	22	11.5	8.5
2)	18	10	8.0
3)	22.5	14	8.5
4)	21	15.5	5.5 ignore

$$\bar{\Delta} = 7.6 \quad \sigma = 1.4$$

$$\text{For 1st 3 } \bar{\Delta} = 8.3 \quad \sigma = .29$$

Test 1/5/82 Load 14.3 kw

Fuel 0% N

	read	0	Δ
1)	40	26	14
2)	41	27	14
3)	41	27.5	13.5

$$\bar{\Delta} = 13.8 \quad \sigma = .289$$

Test 1/6/82 Load - 0

Fuel -0.5% N

	read	0	Δ
1)	10	3	7 ignore
2)	11.5	2	9.5
3)	13	3.5	9.5
4)	13.5	3.5	10
5)	14	4	10
6)	14	4	10

$$\bar{\Delta} = 9.8 \quad \sigma = .27$$

Test 1/6/82 Load 6.25

Fuel 0.5% N

	read	0	Δ
1)	27.5	6.5	21 ignore
2)	30	6	24
3)	31	7	24
4)	31	7	24

Test 1/6/82 Load

Fuel 0.5% N

	read	0	Δ
1)	50	9	41
2)	50	8	42
3)	51	10	41
4)	51	8.25	42.75

NO<sub>x</sub> Values (continued)

5) 32      7.5      24.5

6) 32      7      25

$$\bar{\Delta} = 24.3 \quad \sigma = .45$$

5) 52      10.5      41.5

6) 51.5      9.25      42.25

$$\bar{\Delta} = 41.75 \quad \sigma_{n-1} = .707$$

Test 1/7/82 Load 0

Fuel 1.0% N

	read	0	$\Delta$
	1) 29	6	23
ignore	2) 31	5.5	25.5
	3) 32	7	25
	4) 32	6.5	25.5
	5) 32.5	8	24.5
	6) 33	7.5	25.5
	$\bar{\Delta} = 25.2 \quad \sigma = .45$		

Estimated span drift 5 ppm	$\Delta_{\text{adjusted}} = 30.2 \text{ ppmv}$	$\Delta_{\text{adjusted}} = 51.9 \text{ ppmv}$
span drift 6 ppm		

Test 1/7/82 Load 6.25 Kw

Fuel 1.0% N

	read	0	$\Delta$
	1) 56	11	45
	2) 56	10.5	45.5
	3) 57	12.0	45
	4) 58	11.5	46.5
	5) 59	12.5	46.5
	6) 59	12.0	47
	$\bar{\Delta} = 45.9 \quad \sigma = 8.6$		

Test 1/7/82 Load 15 Kw

Fuel 1.0%

	read	0	$\Delta$
	1) 83	14	69
	2) 83	14	69
	3) 84	15	69
	4) 82	14	68
250 scale ↓	5) 37.25	8.75	71.8
ignore	6) 38	8	75
	$\bar{\Delta} = 68.75 \quad \sigma = 81.5$		

span drift = 13 ppm	$\bar{\Delta}_{\text{adjusted}} = 81.8 \text{ ppm}$

Not likely to be very accurate due to the large span drift

Test 1/8/82 Load 0 Kw

Fuel 1.0%

	read	0	$\Delta$
	1) 28.75	3.0	25.75
	2) 27.0	2.0	25
	3) 28.0	3.0	25
	4) 27.5	2.75	24.75
	5) 28	4.0	24.0
	6) 27.5	3.5	24.0
	$\bar{\Delta} = 24.75 \quad \sigma = .67$		

span drift = 5.5 ppm	$\bar{\Delta}_{\text{adjusted}} = 30.25$

NO<sub>x</sub> Values (continued)

Test 1/8/82 Load 6.25 Kw

Fuel = 1.0% N

Read	0	$\Delta$
1) 48	6.5	41.5
2) 48.5	5.75	42.75
3) 50.5	6.0	44.5
4) 49	5.5	43.5
5) 52	7	45
6) 51	6	45

$$\bar{\Delta} = 43.7 \quad \sigma = 1.4$$

$$\text{span drift} = 4.5 \text{ ppm}$$

$$\Delta_{\text{adjusted}} = 48.2 \text{ ppmv}$$

Test 1/8/82 Load 15.5 Kw

Fuel = 1.0% N

Read	0	$\Delta$	
1) 78	8	70	ignore
2) 77.5	6	71.5	
3) 79.5	7.5	74.5	
4) 78.5	6	72.5	
5) 81	8	73	
6) 80	6	74	

$$\bar{\Delta} = 73.1 \quad \sigma = 1.2$$

$$\text{span drift} = 5.25$$

$$\bar{\Delta}_{\text{adjusted}} = 78.35$$

Test 12/30/81 Load 9.5

Fuel 0% N

Read	0	$\Delta$
1) 16	6.5	9.5
2) 15.5	7	8.5

$$\bar{\Delta} = 9 \quad \sigma = .707$$

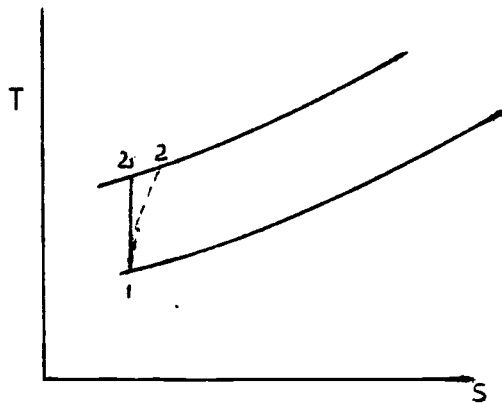
## APPENDIX 7

## Determination of Combustor Inlet Temperature

Assumptions

- 1) Air acts as a perfect gas
- 2) Compressor efficiency is approximately = 80%

The compression process is shown below on a temperature entropy diagram.



1) The initial enthalpy,  $h_1$ , and the entropy at constant pressure,  $\phi_1$ , were obtained by interpolation at actual ambient temperatures on the Keenan and Kaye Gas Tables.<sup>27</sup>

2)  $P_2$  was measured during the run.

3) The isentropic entropy at  $P_2$  was calculated by

$$14 \quad \phi_{2s} = \phi_1 + \frac{R}{J} \ln \frac{P_2}{P_1} = \phi_1 + \frac{1.986 \text{ BTU/lbm}^\circ\text{R}}{28.93 \text{ M.W. Air}} \times \ln \left( \frac{P_2}{P_1} \right)$$

and the corresponding enthalpy,  $h_{2s}$  taken at the same conditions.

4) The actual enthalpy was calculated using the assumed efficiency

$$15 \quad h_2 = \frac{h_{2s} - h_1}{\eta} + h_1$$

and the temperature read from the table at the same conditions.

TABLE VII

## Determination of Combustor Inlet Temperature

Load	Date	Fuel % N	T <sub>in</sub> (°R)	P <sub>in</sub> (atm)	h <sub>1</sub> $\frac{\text{BTU}}{\text{lb}}$	$\phi_1$	P <sub>2</sub> (atm)	$\phi_{2s}$	h <sub>2s</sub> $\frac{\text{BTU}}{\text{lb}}$	h <sub>2</sub>	T <sub>2</sub> °R
0	12/28/81	0.0	513.5	.998	122.71	.58870	2.222	.64365	154.42	162.35	678.42
9	12/28/81	0.0	521.0	.998	124.51	.59219	2.222	.64714	156.69	164.74	688.31
9.5	12/30/81	0.0	521.5	.963	124.63	.59242	2.187	.64873	157.73	166.01	693.57
0	1/5/82	0.0	515.5	1.000	123.19	.58963	2.157	.64240	153.61	161.22	673.71
6.25	1/5/82	0.0	525.0	1.000	125.47	.59402	2.157	.64679	156.46	164.21	686.12
14.3	1/5/82	0.0	532.5	1.000	127.26	.59742	2.225	.65232	160.12	168.34	703.22
0	1/6/82	0.5	507.0	1.015	121.15	.58565	2.239	.63996	152.05	159.78	667.72
6.25	1/6/82	0.5	512.5	1.015	122.47	.58824	2.239	.64255	153.71	161.52	674.96
15.0	1/6/82	0.5	516.5	1.015	123.43	.59010	2.274	.64548	155.60	163.64	683.76
0	1/7/82	1.0	515.5	1.017	123.19	.58963	2.208	.64285	153.90	161.58	675.21
6.25	1/7/82	1.0	522.0	1.017	124.75	.59264	2.242	.64691	156.54	164.49	687.27
15.0	1/7/82	1.0	529.5	1.017	126.54	.59607	2.242	.65034	158.80	166.87	697.14
0	1/8/82	1.0	517.5	1.0167	123.67	.59057	2.207	.64378	154.50	162.21	677.83
6.25	1/8/82	1.0	519.0	1.0167	124.03	.59126	2.241	.64552	155.62	163.52	682.26
15.5	1/8/82	1.0	522.0	1.0167	124.75	.59264	2.241	.64690	156.53	164.48	687.23

## APPENDIX 8

## Weight Percent of an Element in a Fuel Mixture

It is also desirable to know the elemental composition of a fuel mixture when the composition of the various components is known. This can be calculated using equation 12 from Appendix 3.

$$12 \quad \text{Wt \% 1 mix} = \frac{\text{Wt 1}}{\text{Wt Total}} = \frac{\text{Wt \% 1} * (V_1 * \rho_1) + \text{Wt \% 2} * (V_2 * \rho_2)}{(V_1 * \rho_1) + (V_2 * \rho_2)}$$

where:

Wt % 1 mix = weight percent of the desired element in the fuel mixture

Wt Total = Total weight of your fuel mix

Wt % 1 = Weight percent of your element in the fuel additive

$V_1$  = Volume of additive in the fuel mix

$\rho_1$  = Density of the fuel additive

Wt % 2 = Weight percent of the element in your base fuel

$V_2$  = Volume of the base fuel in the final mix

$\rho_2$  = Density of the base fuel

A computer program was written to do this calculation. A copy of the program and the runs for the C, H, and N levels in the fuel mixes used are shown.

## LIST

```

10 REM THIS PROGRAM CALCULATES THE WIEGHT PERCENT OF AN ELEMENT
20 REM IN A FUEL MIXTURE WHEN THE WIEGHT PERCENTS OF THE ELEMENT
30 REM AND THE VOLUMES OF THE CONSTITUANT FUELS ARE KNOWN.
40 !CHR$(27),CHR$(64)
50 !CHR$(12)
60 PRINT " INPUT THE WIEGHT PERCENT OF THE DESIRED ELEMENT IN YOUR "
70 PRINT "ADDITIVE AND THE BASE FUEL.(IN DECIMAL FORM.) "
80 INPUT W1,W2
90 !" "
100 PRINT "INPUT THE DENSITY OF THE ADDITIVE AND THE BASE FUEL."
110 INPUT D1,D2
120 !" "
130 PRINT "INPUT THE NUMBER OF FUEL MIXTURES TO BE CONSIDERED. "
140 INPUT N
150 FOR J=1 TO N
160 !" "
170 PRINT "INPUT THE VOLUME OF THE ADDITIVE AND THE BASE FUEL. "
180 INPUT V1,V2
190  $W=(W1*V1*D1+W2*V2*D2)/(V1*D1+V2*D2)$ 
200 !" "\!" "
210 PRINT "THE WIEGHT PERCENT OF THE FINAL MIX IS: ",W*100.0," %"
220 !" "\!" "
230 NEXT J
PRESS RETURN TO CONTINUE
240 END
READY

```

6                   Kerosene Pyridine Mixtures C%  
 INPUT THE WIEGHT PERCENT OF THE DESIRED ELEMENT IN YOUR  
 ADDITIVE AND THE BASE FUEL.(IN DECIMAL FORM.)  
 1.7556, .90645

INPUT THE DENSITY OF THE ADDITIVE AND THE BASE FUEL.  
 1.9765,.7934

INPUT THE NUMBER OF FUEL MIXTURES TO BE CONSIDERED.  
 13

INPUT THE VOLUME OF THE ADDITIVE AND THE BASE FUEL.  
 10.0,18926.65

THE WIEGHT PERCENT OF THE FINAL MIX IS: 90.645004 %

INPUT THE VOLUME OF THE ADDITIVE AND THE BASE FUEL.  
 1433.5,184930.1

THE WIEGHT PERCENT OF THE FINAL MIX IS: 90.221983 %

INPUT THE VOLUME OF THE ADDITIVE AND THE BASE FUEL.  
 1871.6,18035. 0.5% N

THE WIEGHT PERCENT OF THE FINAL MIX IS: 89.796987 %1.0%N

6                   %N  
 INPUT THE WIEGHT PERCENT OF THE DESIRED ELEMENT IN YOUR  
 ADDITIVE AND THE BASE FUEL.(IN DECIMAL FORM.)  
 1.17830,0,0.0

INPUT THE DENSITY OF THE ADDITIVE AND THE BASE FUEL.  
 1.9765,.7934

INPUT THE NUMBER OF FUEL MIXTURES TO BE CONSIDERED.  
 13

INPUT THE VOLUME OF THE ADDITIVE AND THE BASE FUEL.  
 10.0,18926.65

THE WIEGHT PERCENT OF THE FINAL MIX IS: 0 %

INPUT THE VOLUME OF THE ADDITIVE AND THE BASE FUEL.  
 1433 .5,18493.1

THE WIEGHT PERCENT OF THE FINAL MIX IS: .49998654 % .5%N

INPUT THE VOLUME OF THE ADDITIVE AND THE BASE FUEL.  
 1871.6,18035

THE WIEGHT PERCENT OF THE FINAL MIX IS: .99996501 %1.0%N

## Kerosene Pyridine Mixtures %H

6  
 INPUT THE WIEGHT PERCENT OF THE DESIRED ELEMENT IN YOUR  
 ADDITIVE AND THE BASE FUEL.(IN DECIMAL FORM.)  
 1.0661,.09355

INPUT THE DENSITY OF THE ADDITIVE AND THE BASE FUEL.  
 1.9765,.7934

INPUT THE NUMBER OF FUEL MIXTURES TO BE CONSIDERED.  
 13

INPUT THE VOLUME OF THE ADDITIVE AND THE BASE FUEL.  
 10.0,18926.65

THE WIEGHT PERCENT OF THE FINAL MIX IS: 9.355 %

INPUT THE VOLUME OF THE ADDITIVE AND THE BASE FUEL.  
 1433.5,18493.1

THE WIEGHT PERCENT OF THE FINAL MIX IS: 9.2780247 % 0.5%N

INPUT THE VOLUME OF THE ADDITIVE AND THE BASE FUEL.  
 1871.6,18055.

THE WIEGHT PERCENT OF THE FINAL MIX IS: 9.2010519 % 1.0%N

## APPENDIX 9

## Fuel Density Calculations

T ambient = 75°F

Measured 9/3/81

API gravities were calculated from the measured densities adjusted to 60°F.

Volume coefficients of expansion for petroleum fuels are:<sup>28</sup>

API	Coefficient $\frac{\Delta \text{Volume}}{\Delta T ^\circ\text{F}}$
Below 14.9	0.00035
15 - 34.9	.0004
35 - 50.9	.0005

Density of H<sub>2</sub>O

$$\rho_{\text{H}_2\text{O}} = .99905 \text{ g/ML}^{29}$$

## CALCULATIONS

$$1. \text{ Kerosene: } 25 \text{ ML} = 40.0798 \text{ g} - 20.2442 \text{ g} = 19.8356 \text{ g}$$

container

$$16 \quad \rho = \frac{\text{mass measured}}{\text{volume measured}}$$

a) at T<sub>amb</sub>

$$\rho = \frac{19.8356 \text{ g}}{25 \text{ ML}} = \underline{.7934 \text{ g/ML}} \left( \frac{\text{Kg}}{\text{L}} \right) \left( \frac{\text{L}}{\text{L}} \right) * 8.3452 \frac{\frac{16}{\text{gal}}}{\frac{\text{Kg}}{\text{L}}} = 6.6210 \frac{1\text{b}}{\text{gal}}$$

b) at 60°F

$$\rho = \frac{19.8356 \text{ g}}{25 \text{ ML} + (25 * .0005 * -15^\circ\text{F}) \text{ ML}} = \underline{.7994 \frac{\text{g}}{\text{ML}}} \left( \frac{\text{kg}}{\text{L}} \right) [6.6713 \frac{1\text{b}}{\text{gal}}]$$

c) Specific gravity at 60°F (S)

$$17 \quad S = \frac{\rho_{\text{fuel}} (60^\circ\text{F})}{\rho_{\text{H}_2\text{O}} (60^\circ\text{F})} = \frac{.7994}{.99905} = \underline{.8002}$$

## 1. Kerosene

## d) API Gravity

$$18 \quad \text{API} = \frac{141.5}{S} - 131.5$$

$$\underline{\text{API}} = \frac{141.5}{.8002} - 131.5 = \underline{45.3308}$$

$$2. \text{ Toluene } 25 \text{ ML} = 41.5338 \text{ g} - 20.1198 \text{ g} = 21.4140 \text{ g}$$

a) at  $T_{\text{amb}}$ 

$$\rho = \frac{21.4140 \text{ g}}{25 \text{ ML}} = \underline{.8566 \frac{\text{g}}{\text{ML}} \left( \frac{\text{kg}}{\text{L}} \right)} [7.1483 \frac{\text{lb}}{\text{gal}}]$$

b) at  $60^{\circ}\text{F}$ 

$$\rho = \frac{21.4140 \text{ g}}{25 + (25 * .0004 * -15^{\circ}\text{F})} = \underline{.8617 \frac{\text{g}}{\text{ML}} \left( \frac{\text{kg}}{\text{L}} \right)} [7.1913 \frac{\text{lb}}{\text{gal}}]$$

c) Specific gravity at  $60^{\circ}\text{F}$ 

$$S = \frac{.8617}{.99905} = \underline{.8625}$$

## d) API Gravity

$$\underline{\text{API}} = \frac{141.5}{.8625} - 131.5 = \underline{32.5580}$$

## 3. Pyridine

$$a) \text{ at } T_{\text{amb}} \quad 25 \text{ ML} = 43.9950 \text{ g} - 19.5813 \text{ g} = 24.4137 \text{ g}$$

$$\rho = \frac{24.4137 \text{ g}}{25 \text{ ML}} = \underline{.9765 \frac{\text{g}}{\text{ML}} \left( \frac{\text{kg}}{\text{L}} \right)} [8.1490 \frac{\text{lb}}{\text{gal}}]$$

b) at  $60^{\circ}\text{F}$ 

$$\rho = \frac{24.4137 \text{ g}}{25 + (25 * .00035 * -15^{\circ}\text{F})} = \underline{.9817 \frac{\text{g}}{\text{ML}} \left( \frac{\text{kg}}{\text{L}} \right)} [8.1925 \frac{\text{lb}}{\text{gal}}]$$

c) Specific Gravity at 60°F

$$S = \frac{.9817}{.99905} = \underline{.9826}$$

d) API Gravity

$$\underline{API} = \frac{141.5}{.9826} - 131.5 = \underline{12.5057}$$

### Accuracy of Density Measurements

a) Temperature Variation

i) The maximum change in the density of kerosene for the temperature range encountered was 1.58% when the ambient temperature reached 44°F

$$\Delta \rho \text{ kerosene } 44^\circ\text{F} = \frac{.8059 - .7934}{.7934} = .01577 \text{ (1.58\%)}$$

ii) The density ratio change for kerosene and pyridine  $\frac{\rho_p}{\rho_k}$  was

$$20 \quad = \frac{\left(\frac{.9873}{.8059}\right) - \left(\frac{.9765}{.7934}\right)}{\left(\frac{.9765}{.7934}\right)} = -.0046 \text{ (-.46\%)}$$

Therefore for mixing fuels this error can be considered negligible.

b) Investigation of density changes for the various fuel mixtures.

Compare the 1% N mix and pure kerosene at 60°F.

$$\begin{aligned} \rho_{\text{mix}} &= \frac{\rho_p V_p + \rho_k V_k}{V_{\text{Total}}} \\ &= \frac{.9817 \text{ g/ML} * 871.6331 \text{ g/ML} + .7994 \text{ g/ML} * 18055.017 \text{ ML}}{18926.85 \text{ ML}} \\ &= .8078 \text{ g/ML} \end{aligned}$$

$$\Delta \rho = \frac{.8078 - .7994}{.7994} = .0105 \text{ (1.05\%)}$$

For the purposes to which these values are put (i.e. calculation of A/F ratios), this error is negligible in comparison with the inaccuracies associated with the air flow measurements.

However, if the fuel flow is known accurately, a comparison of the A/F ratios calculated directly with the A/F ratios calculated using CO and CO<sub>2</sub> measurements will give an idea of the accuracy of the air flow measurements.

For this reason a determination of the actual fuel densities for each run was made, assuming that the fuel remained at the initial ambient temperature for that day. These values are given in the following table.

TABLE VIII

## Fuel Densities Used

Date	Fuel	Tdb Ambient Temp °F	Density g/ML ( $\frac{\text{kg}}{\text{L}}$ )
12/28/81	100%K 0.0% N	50	.8035
12/30/81	100%K 0.0% N	54	.8018
1/5/82	100%K 0.0% N	51	.8031
1/6/82	0.5% N	44	.8101
1/7/82	1.0% N	52	.8110
1/8/82	1.0% N	57	.8090

## APPENDIX 10a

## Calculation of A/F Ratios by Direct Measurement

As a check on our calculations based on CO and CO<sub>2</sub> measurements, it was decided to calculate the air fuel ratios directly from measured variables. Shown below is a derivation of those equations necessary to achieve this end.

## A. Calculation of Exhaust Mass Flow Rate

## 1) Assumptions

- a) The exhaust is treated as a perfect gas with the properties of air
- b) The exhaust is at atmospheric pressure

2) The following derivations were taken from literature supplied by the F.W. Dwyer Mfg. Co., Inc.<sup>30</sup>

## 3) Air Velocity

$$22 \quad V_{el} = 1096.2 (P_v/D)^{\frac{1}{2}} \quad [\text{ft/min}]$$

$P_v$  = velocity pressure [in. H<sub>2</sub>O]

$D$  = Air density [lb/ft<sup>3</sup>]

## 4) Air Density

$$23 \quad D = 1.325 * \frac{P_b}{T} \quad [\text{lb/ft}^3]$$

$P_b$  = barometric pressure

$T$  = temperature °R (°F + 460)

## 5) Mass Flow Rate

$$\begin{aligned}
 24 \quad \dot{M}_E &= \text{velocity} [\text{ft/min}] * \text{Duct Area} [\text{ft}^2] * \text{density} [\text{lb/ft}^3] \\
 &= 1096.2 * (P_v/D)^{\frac{1}{2}} * D * A \\
 &= 1096.2 * (P_v * D)^{\frac{1}{2}} * A \\
 &= 1096.2 * (P_v * (1.325 * P_b/T))^{\frac{1}{2}} * \left( \frac{5}{12} \right)^2 \frac{1}{4}
 \end{aligned}$$

Direct A/F measurement (continued)

$$25 \quad \dot{M}_E = 149.4711 * (P_v * (1.325 * P_B / T))^{\frac{1}{2}} \quad [\text{lb/min}]$$

B. Calculation of Fuel Mass Flow Rate

1) Assumption:

a) That the flow rate was essentially constant.

2) The measured value was seconds per 2000 cc.

This value was converted into mass flow rate in lb/min.

$$\begin{aligned} \dot{M}_F &= \frac{2000}{t_f} \left[ \frac{\text{cc}}{\text{sec}} \right] * D_f \left[ \frac{\text{kg}}{\text{cc}} \right] * \frac{1}{1000} \left[ \frac{\text{L}}{\text{cc}} \right] * \frac{1}{.4535} \left[ \frac{\text{lb}}{\text{kg}} \right] * 60 \left[ \frac{\text{sec}}{\text{min}} \right] \\ 26 \quad &= 263.1579 * \frac{D_F}{T_F} \quad \text{lb/min} \end{aligned}$$

C. The Air Fuel Ratio can then be calculated by

The mass ratio

$$27 \quad A/F = \frac{\dot{M}_E - \dot{M}_F}{\dot{M}_F}$$

D. The values calculated are shown in Table IX. The values calculated by CO and CO<sub>2</sub> measurements are also shown for comparison.

Table 9

Calculation of A/F ratios by Direct Measurement  
Compared to those Calculated from CO<sub>2</sub>

$$\dot{M}_E = 149.4711 * \sqrt{P_v} * (1.325 * P_B/T) \quad \left[ \frac{\text{lb}}{\text{min}} \right]$$

$$\dot{M}_F = 263.1579 * \frac{O_F \left[ \frac{\text{kg}}{\text{L}} \right]}{t_T \left[ \text{s} \right]} \quad \left[ \frac{\text{lb}}{\text{min}} \right]$$

$$A/F = \frac{\dot{M}_E - \dot{M}_F}{\dot{M}_F}$$

	Fuel	Load	Pv	Pb in Hg	T°R <sub>exh</sub>	$\frac{\text{lb}}{\text{min}}$ M <sub>E</sub>	DF	t <sub>F</sub> sec	$\frac{\text{lb}}{\text{min}}$ M <sub>F</sub>	A/F <sub>M</sub>	A/F <sub>D</sub> *
12/28/81	100%K 0%N	9 kw	5.3	29.85	1115	64.8094	.8035	338.	.62558	102.599	100.62*
12/28/81	100%K 0%N	0 kw	3.8	29.85	920	60.4137	.8035	462.	.45768	131.000	145.35
1/5/82	100%K 0%N	0 kw	V [1500] [1664] [1882]	29.93	928	64.1012	.8031	476.5	.44353	143.525	140.350
1/5/82	100%K 0%N	6.25 kw		29.93	1071	61.6150	.8031	380.	.55616	109.786	108.503
1/5/82	100%K 0%N	14.3 kw		29.93	1277	58.4455	.8031	284	.74416	77.539	77.817
1/6/82	0.5%N	0 kw	3.9	30.36	911	65.2541	.8101	471.2	.45243	143.230	145.348
1/6/82	0.5%N	6.25 kw	4.8	30.36	1043	67.6571	.8101	375.6	.56758	118.203	111.478
1/6/82	0.5%N	15 kw	5.4	30.36	1224	66.2432	.8101	283.1	.75304	86.968	81.756
1/7/82	1.0%N	0 kw	3.9	30.43	925	61.6279	.8110	469.1	.45496	134.458	142.805
1/7/82	1.0%N	6.25 kw	4.3	30.43	1068	60.2233	.8110	375.1	.56897	104.846	109.971
1/7/8	1.0%N	15 kw	5.0	30.43	1245	60.1473	.8110	290.1	.73568	80.757	77.817
1/8/82	1.0%N	0 kw	4.1	30.42	930	63.0079	.8090	470.0	.45296	138.103	142.805
1/8/82	1.0%N	6.25 kw	4.3	30.42	1063	60.3549	.8090	377.5	.56396	106.020	108.503
1/8/82	1.0%N	15.5 kw	5.3	30.42	1248	61.8408	.8090	285.7	.74517	81.989	78.575
12/30/81	100% 0%N	9.5 kw	4.8	28.8	1131	60.1521	.8018	330 <sup>(est)</sup>	.63939	93.077	99.69*

\* Calculated using the equation  
derived for kerosene as no  
CO data was available.

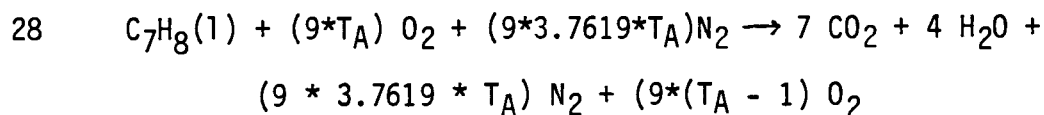
## APPENDIX 10b

Calculation of the Percent Theoretical Air in Combustion  
from Combustion Stoichiometry

## A. Assumptions:

- 1) Complete combustion
- 2) No appreciable disassociation of the combustion products

## B. Chemical Reaction Equation (for pure Toluene)



$T_A$  = Percent theoretical air expressed as a decimal

C. Vol % CO<sub>2</sub> Calculation

$$29 \quad 1) \% \text{CO}_2 = \frac{\text{Mol CO}_2}{\text{Mol CO}_2 + \text{Mol H}_2\text{O} + \text{Mol N}_2 + \text{Mol O}_2}$$

$$2) \% \text{CO}_2 = \frac{7}{7 + 4 + (9 \cdot 3.7619 \cdot T_A) + 9 \cdot (T_A - 1)}$$

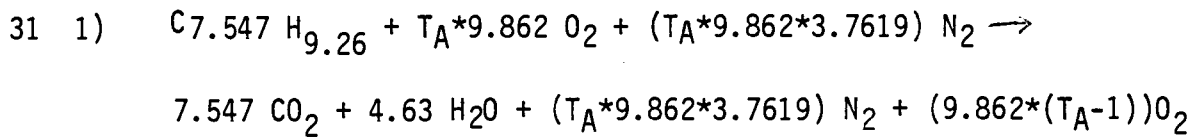
$$= \frac{7}{11 + T_A \cdot (9 \cdot 3.7619 + 9) - 9}$$

$$= \frac{7}{2 + T_A \cdot (42.8571)}$$

$$3) 2 + T_A \cdot (42.8571) = \frac{7}{\% \text{CO}_2}$$

$$30 \quad 4) T_A = \left( \frac{7}{\% \text{CO}_2} - 2 \right) \cdot \frac{1}{42.8571}$$

#### D. Modification of Theoretical Air Calculations to fit Kerosene's Composition



$$2) \quad \% CO_2 = \frac{7.547}{7.547 + 4.63 + (9.862 * 3.7619 * T_A) + (9.862 * (T_A - 1))}$$

$$= \frac{7.547}{12.177 + T_A (9.862 * 3.7619 + 9.862) - 9.862}$$

$$= \frac{7.547}{2.315 + T_A (46.9619)}$$

$$32 \quad 3) \quad T_A (\text{kerosene}) = \left( \frac{7.547}{\% CO_2} - 2.315 \right) * \frac{1}{46.9619}$$

These calculations can be converted to the air fuel ratio by multiplying by the Stoichiometric air fuel ratio for the specific fuel in question.

For kerosene this is found by the following calculation:

$$33 \quad \frac{\text{Mass Air}}{\text{Mass Fuel}} = \frac{(9.862 * 32.00) + (9.862 * 3.7619 * 28.016)}{(7.547 * 12.01) + (9.26 * 1.01)}$$

$$= 13.55$$

#### E. Accuracy

The accuracy of the above calculations are highly dependent on the actual chemical composition of the fuel and the accuracy of the original assumptions.

While searching the literature a method recommended by The Society of Automotive Engineers was found. As this method is an industrial standard, it was used in most cases in place of our derived equations.

Because of the good correlation between this method and that obtained by direct measurement, (see Appendix 10a), an accuracy of  $\pm 3$  in the A/F ratios seems reasonable for this method.

## APPENDIX 11

## Calculation of Heat of Formation of Kerosene

## A. High Heating Value

$$34 \quad \text{HHV} \left( \frac{\text{BTU}}{\text{lb}} \right) = 18,440 + 40 (\text{API}-10) \\ (\text{Sherman and Kropff equation modified})^{31}$$

For kerosene

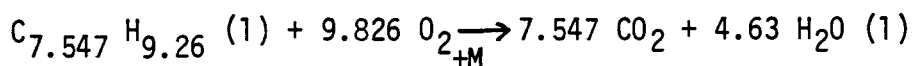
$$\text{HHVL} = 18,440 + 40 (45.3308-10) = 19,853 \frac{\text{BTU}}{\text{lb}}$$

## B. Accuracy

The text from which the above equation was taken states "[It is] probably more accurate than would be obtained by an inexperienced operator using a Bomb Calorimeter"<sup>32</sup>. As a comparison the 21st edition of The Handbook of Physics and Chemistry (pg. 1032), gives a value of  $19,810 \frac{\text{BTU}}{\text{lb}}$  as the heat of combustion of kerosene.

In light of the above two facts, it seems reasonable to assume that the derived value is accurate to within  $75 \frac{\text{BTU}}{\text{lb}}$ .

## C. Heat of Formation



$$35 \quad \text{HHV} = \left[ \sum \text{H}_f \text{ Products} - \sum \text{H}_f \text{ Reactants} \right]$$

$$\sum \text{H}_f \text{ Reactants} = \sum \text{H}_f \text{ Products} + \text{HHV}$$

$$\sum \text{H}_f \text{ Reactants} = \sum \text{H}_f \text{C}_{7.547} \text{H}_{9.26} + \text{H}_f \text{O}_2 \rightarrow \emptyset$$

$$\Sigma H_f = (7.547 \times -393,520 \frac{\text{kJ}}{\text{Kg mol}}) + (4.63 \times -285,830 \frac{\text{kJ}}{\text{Kg mol}})$$

Products  $\text{CO}_2(\text{g})$   $\text{H}_2\text{O}(\text{l})$

$$= -4,293,288$$

$$\text{HHV}^{(\text{L})} = 19,853 \frac{\text{BTU}}{\text{lb}} * 1054.8 \frac{\text{J}}{\text{BTU}} * \frac{1 \text{ lb}}{453.5924 \text{ g}} * \overbrace{\frac{100 \text{ g}}{\text{g mol}}}^{\text{MW}} * \frac{1000}{1000}$$

$$= 4,616,687.7 \frac{\text{kJ}}{\text{Kg mol}} * 1 \text{ mol} =$$

$$4,616,687.7 \text{ kJ}$$

$$H_f^{(1)} = 4,616,687.7 + -4,293,288$$

$$\text{C}_{7.547} \text{H}_{9.26} = 323,399 \text{ kJ}$$

## APPENDIX 12

## Estimate of the Adiabatic Flame Temperature

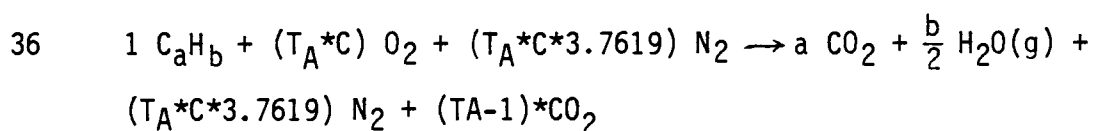
## A. Assumptions

- 1) That the air can be accurately modeled as a mixture of nitrogen and oxygen containing 79% N<sub>2</sub> and 21% O<sub>2</sub>.
- 2) That complete combustion occurs.

This is a normal assumption for adiabatic flame temperature calculations. The assumption is considered good for gas turbine combustors where normally a minimum of 400% excess air is supplied. Measured values of CO were at most 640 ppmv (0.064% by volume), while NO<sub>x</sub> values for the pure nitrogen free fuels topped out at about 17 ppmv (.0017% by volume). The presence of these compounds was therefore considered too small to significantly effect the outcome of these calculations.

## B. Chemical Formula

The equation used for this derivation was that of a pure hydrocarbon.



where:

a - moles of carbon

b - moles of hydrogen

c - "moles" of air

T<sub>A</sub> - Percent theoretical air expressed as a decimal



b) That the increase in pressure of the air and fuel had a negligible effect on their enthalpy.

c) That the incoming thermal enthalpy of the fuel is negligible. i.e.  $T = 298\text{K}$ .

2) The Datum for this calculation was taken as  $298\text{K}$  at one atmosphere to correlate with the JANAF Tables.

$$3) 4.186 \frac{\frac{\text{kJ}}{\text{g mol}}}{\frac{\text{k cal}}{\text{g mol}}} * \left\{ \begin{array}{l} \text{Products} \\ [7.596 \text{ mol CO}_2 * (-94.054 \frac{\text{k cal}}{\text{mol}} + h_T \frac{\text{k cal}}{\text{mol}} - 0)] \end{array} \right.$$

$$k_{\text{cal}} + [4.329 \text{ mol H}_2\text{O(g)} * (-57.798 \frac{\text{k cal}}{\text{mol}} + h_T \frac{\text{k cal}}{\text{mol}} - 0)] k_{\text{cal}} + \\ [(9.7605 * 3.7619 * T_A) \text{ mol N}_2 * (0 + h_T - 0)] k_{\text{cal}} + [(T_A - 1) * 9.7605 \text{ mol O}_2 \\ * (0 + h_T - 0)] k_{\text{cal}} \} \text{ kJ}$$

$$\text{kJ} = [1 \text{ mol Toluene} * (12.008 \frac{\text{kJ}}{\text{g mol}} + 0 - 0)] \text{ kJ} + \\ \text{Reactants}$$

$$4.186 \frac{\frac{\text{kJ}}{\text{g mol}}}{\frac{\text{k cal}}{\text{g mol}}} * \left\{ \begin{array}{l} [(9.7605 * T_A) \text{ mol O}_2 * (0 + h_T - 0)] k_{\text{cal}} \\ + [(9.7605 * 3.7619 * T_A) \\ \text{mol N}_2 * (0 + h_T - 0)] k_{\text{cal}} \end{array} \right\} \text{ kJ}$$

4a) For  $T_A = 1$  (Stoichiometric A/F Ratio)

$$(-2990.6215 \text{ kJ} + 31.7969 h_T \text{ kJ})_{\text{CO}_2} + (-1047.3688 + 18.1212 h_T \text{ kJ})_{\text{H}_2\text{O}} \\ \text{Products}$$

$$+ (153.7017 h_T \text{ kJ})_{\text{N}_2} = \text{Reactants} \quad 12.008 \text{ kJ} + (40.8575 h_T \text{ kJ})_{\text{O}_2}$$

$$+ (153.7017 h_T \text{ kJ})_{\text{N}_2}$$

$$\begin{aligned}
 4b) \quad & 31.7967 h_{T_p} \text{CO}_2 \text{ kJ} + 18.1212 h_{T_p} \text{H}_2\text{O(g)} \text{ kJ} + 153.7017 h_{T_p} \text{N}_2 \\
 & = 4049.9983 \text{ kJ} + 40.8575 h_{T_R} \text{O}_2 \text{ kJ} + 153.7017 h_{T_{RN_2}} \text{ kJ}
 \end{aligned}$$

5) The  $\text{NO}_x$  values have been adjusted to combustor inlet temperatures of  $100^\circ\text{C}$ . Therefore, the enthalpies of the air components are taken at this temperature

$$\begin{aligned}
 & (31.7967 h_{T_p} \text{CO}_2 + 18.1212 h_{T_p} \text{H}_2\text{O(g)} + 153.7017 h_{T_p} \text{N}_2) \text{ kJ} \\
 & = [4049.9983 + (40.8575 \cdot 533^1)_{\text{O}_2} + (153.7017 \cdot 5229)_{\text{N}_2}] \text{ kJ} \\
 & = 4152.1501 \text{ kJ}
 \end{aligned}$$

6) As a rough approximation we will ignore the water and carbon dioxide and solve directly for  $h_{T_p} \text{N}_2$ .

$$h_{T_p} \text{N}_2 = \frac{4152.1501 \text{ kJ}}{153.7017 \left( \frac{\text{kJ}}{\text{kcal}} \right)} = 27.0143 \frac{\text{kcal}}{\text{mol}}$$

From the charts  $T = 3540 \text{ K}$

7) We will now approach the more accurate solution.

$T^\circ\text{K}$	$H_T \text{CO}_2$	$H_T \text{H}_2\text{O}$	$H_T \text{N}_2$	$H_T \text{O}_2$	$\Delta(H_{T_{\text{O}_2}} - H)$
2500	29.141	23.653	17.761	4085.104	-66.7740
2600	30.613	24.945	18.638	4290.118	+137.9679

Linear interpolation between these values gives  $2532.6\text{K}$  ( $4099.0^\circ\text{F}$ )

## E. Computer Program

A program was written to assist in the solution of these equations. A copy of the program follows. This program was run for Toluene to verify that the results match. Once this run was completed, a series of runs for kerosene were made matching the inlet nitrogen and oxygen temperature enthalpies with actual test conditions. These were then used in Table I.

The program was also run with average theoretical air values for graphing purposes in the Results section.

For a discussion of the accuracy of these calculations, see the discussion on the Adiabatic Flame Temperature in the Results section.

LIST

```

10 !CHR$(27),CHR$(64)
20 !CHR$(12)
30 !" THIS PROGRAM ASSISTS IN SOLVING THE ADIABATIC FLAME TEMPERATURE "
40 !" EQUATION FOR THE COMBUSTION OF A PURE HYDROCARBON. THE CHEMICAL "
50 !" FORMULA FOR THIS REACTION IS:"
60 !"  $C_aH_b(L) + (TA*c)O_2 + (TA*c*3.7619)N_2 = aCO_2 + (b/2)H_2O(G) + (TA*c*3.7619)N_2 +$ ,
70 !"  $(c*(TA-1))O_2$ "
80 !" NOTE: A NEGATIVE DIFFERENCE INDICATES TOO LOW A GUESS AND VICE VERSA."
90 !" THE PROGRAM WILL INTERPOLATE BETWEEN YOUR LAST TWO GUESSES."
100 REM
110 DIM D(6,7)
120 !\!\PRINT "INPUT THE MOLES OF CARBON AND HYDROGEN IN THE FUEL (a AND b)"
130 INPUT M1,M2
140 M3=M1+(M2/4) \ REM MOLES OF AIR
150 PRINT "INPUT THE HEAT OF FORMATION OF THE FUEL IN KJ/GRAM MOLE. "
160 INPUT F1
170 !" ENTER THE PERCENT THEORETICAL AIR AS A DECIMAL"
180 INPUT A
190 A9=A
200 PRINT " INPUT THE INLET AIR TEMPERATURE AND THE CORRESPONDING O2 AND ",
210 PRINT "N2 ENTHALPIES."
220 INPUT T,O2,N2
230 !\!\!
PRESS RETURN TO CONTINUE
240 REM TEMPERATURE ITERATION LOOP
250 FOR J=1 TO 6
260 PRINT " INPUT THE ESTIMATED TEMPERATURE AND ",
270 PRINT " THE ENTHALPY VALUES FOR CO2,"
280 PRINT "H2O,N2,,O2. ENTER ZERO'S ",
290 PRINT " TO END BEFORE THE 6' TH ITERATION."
300 INPUT D(J,1),D(J,2),D(J,3),D(J,4),D(J,5)
310 IF D(J,1)=0. THEN GOTO 530
320 REM
330 REM CALCULATION OF TOTAL ENTHALPY
340 B=(1*F1)
350 C=(4.186*M1*94.054)
360 D=(4.186*(M2/2)*57.798)
370 F=4.186*M3*A*O2 \ REM THERMAL ENTHALPIY OF ENTERING OXYGEN
380 G=4.186*M3*3.7619*A*N2 \ REM THERMAL ENTHALPY OF ENTERING NITROGEN
390 H=B+C+D+F+G
400 REM
410 REM CALCULATION OF TOTAL TEMPERATURE ENTHALPIES
420 H2=(M1*D(J,2))
430 H3=((M2/2)*D(J,3))
440 H4=(A*M3*3.7619*D(J,4))
450 H5=(M3*(A-1)*D(J,5))
460 D(J,6)=4.186*(H2+H3+H4+H5)
PRESS RETURN TO CONTINUE
470 REM
480 REM CALCULATION OF CLOSENESS OF APPROXIMATION
490 D(J,7)=D(J,6)-H
500 PRINT "THE DIFFERENCE IS: ",D(J,7)
510 PRINT " "
520 PRINT " "
530 NEXT J
540 REM OUTPUT
550 PRINT " \!" "

```

```

560 !" THE PERCENT THEORETICAL AIR IS: ",A9*100.0
570 !"THE INLET AIR TEMPERATURE IS: ",T\!\!
580 PRINT " T(K)          HTO2          HTH20          HTN2          HTO2          ",
590 PRINT "HT TOT      (HTTOT-H)"
600 PRINT " "
610 FOR K=1 TO (J-1)
620 PRINT XZ9F3,D(K,1),XZ11F3,D(K,2),D(K,3),D(K,4),D(K,5),D(K,6),D(K,7)
630 NEXT K
640 K=J-1
650 REM
660 REM LINEAR INTERPOLATION
670 REM
680 IF D(K,7)>0.0 THEN GOTO 740
690 A=D(K,1)\ REM LOW TEMP
PRESS RETURN TO CONTINUE
700 B=D(K,7)\ REM LOW DIFFERENCE
710 C=D((K-1),1)\ REM HIGH TEMP.
720 D=D((K-1),7)\ REM HIGH DIFFERENCE
730 GOTO 780
740 A=D((K-1),1)\ REM LOW TEMP
750 B=D((K-1),7)\ REM LOW DIFFERENCE
760 C=D(K,1)\ REM HIGH TEMP.
770 D=D(K,7)\ REM HIGH DIFFERENCE
780 E=(ABS(B)/(D-B))*(C-A)+A\ REM INTERPOLATED TEMPERATURE
790 E2=((E-273.15)*(9.0/5.0))+32.0\ REM K TO DEGREES F CONVERSION
800 !\!\!
810 PRINT"          INTERPOLATION "
820 !\PRINT" T(K)          (HTOT-H)"
830 !\!\PRINT" ",XZ9F3,A," ",XZ9F3,B
840 !\!" ",XZ9F3,C," ",XZ9F3,D
850 !\!\!"THE INTERPOLATED TEMPERATURE IS: ",E," K (",E2," F)"
860 END
READY

```

Toluene

THIS PROGRAM ASSISTS IN SOLVING THE ADIABATIC FLAME TEMPERATURE EQUATION FOR THE COMBUSTION OF A PURE HYDROCARBON. THE CHEMICAL FORMULA FOR THIS REACTION IS:

$$C_aH_b(L) + (TA \cdot c)O_2 + (TA \cdot c \cdot 3.7619)N_2 = aCO_2 + (b/2)H_2O(G) + (TA \cdot c \cdot 3.7619)N_2 + (c \cdot (TA - 1))O_2$$

NOTE: A NEGATIVE DIFFERENCE INDICATES TOO LOW A GUESS AND VICE VERSA. THE PROGRAM WILL INTERPOLATE BETWEEN YOUR LAST TWO GUESSES.

INPUT THE MOLES OF CARBON AND HYDROGEN IN THE FUEL (a AND b)  
 ?7.596,8.658  
 INPUT THE HEAT OF FORMATION OF THE FUEL IN KJ/GRAM MOLE.  
 ?12.008  
 ENTER THE PERCENT THEORETICAL AIR AS A DECIMAL  
 ?1.00  
 INPUT THE INLET AIR TEMPERATURE AND THE CORRESPONDING O2 AND N2 ENTHALPIES.  
 ?373.15,.5331,.5229

INPUT THE ESTIMATED TEMPERATURE AND THE ENTHALPY VALUES FOR CO2, H2O, N2, O2. ENTER ZERO'S TO END BEFORE THE 6'TH ITERATION.  
 ?2500,29.141,23.653,17.761,18.732  
 THE DIFFERENCE IS: -67.0421

INPUT THE ESTIMATED TEMPERATURE AND THE ENTHALPY VALUES FOR CO2, H2O, N2, O2. ENTER ZERO'S TO END BEFORE THE 6'TH ITERATION.  
 ?2600,30.613,24.945,18.638,19.664  
 THE DIFFERENCE IS: 137.9717

INPUT THE ESTIMATED TEMPERATURE AND THE ENTHALPY VALUES FOR CO2, H2O, N2, O2. ENTER ZERO'S TO END BEFORE THE 6'TH ITERATION.  
 ?0.0,0.0,0.0,0.0,0.0

THE PERCENT THEORETICAL AIR IS: 100  
 THE INLET AIR TEMPERATURE IS: 373.15

T(K)	HTCO2	HTH2O	HTN2	HTO2	HT TOT	(HTTOT-H)
2500.	29.141	23.653	17.761	18.732	4085.108	-67.042
2600.	30.613	24.945	18.638	19.664	4290.122	137.972

#### INTERPOLATION

T(K)	(HTTOT-H)
2500.	-67.042
2600.	137.972

THE INTERPOLATED TEMPERATURE IS: 2532.7013 K ( 4099.1923 F )  
 READY